Multiphoton Exchange Amplitudes at Infinite Energy

SHAU-JIN CHANG* AND SHANG-KENG MA†
Institute for Advanced Study, Princeton, New Jersey 08540
(Received 3 June 1969)

We illustrate in detail the summation of multiphoton exchange diagrams for ee, γe, and $\gamma\gamma$ elastic scattering amplitudes at the high-energy limit using the infinite-momentum technique reported earlier. These diagrams are shown to give rise to amplitudes proportional to s, the center-of-mass energy squared, multiplied by simple combinations of the eikonal forms of high-energy scattering.

I. INTRODUCTION

MUCH work has been done on the theory of elastic two-body scattering in the infinite-energy limit. Qualitative forms of the scattering amplitude at infinite s and finite t have been proposed based on the Regge model and the eikonal or diffraction model,[1] which is related to the droplet model of Chou and Yang.[2] The predictions of these models seem to be consistent with the well-established fact that the forward ($t=0$) scattering amplitudes for hadrons tend to s as $s\to\infty$.

These models are built on extrapolations from the nonrelativistic potential scattering theory instead of relativistic first principles. Because of this fact, explicit calculations based on relativistic field theories are of great interest. Some work has already been done along this line. For example, the Regge behavior has been shown to appear in the scalar-meson theory when the ladder diagrams in the t channel are summed.[3] Torgerson has analyzed the charged scalar-meson scattering up to three-photon exchange in the s channel and found the result consistent with the eikonal approximation.[1] More recently, Cheng and Wu have studied thoroughly the lowest-order diagrams in quantum electrodynamics (QED) and found the scattering amplitudes to be proportional to s as $s\to\infty$.[4] In the case of the scattering of a photon by the static Coulomb field of a nucleus of charge Z, i.e., the Delbrück scattering, they have studied the amplitude to all orders in Z.

In studying a field-theory model, one hopes that the high-energy behavior of the scattering amplitudes derived from the model might turn out to be relevant to hadron physics. Therefore, one must extract from the model those general features which are not based on any finite-order perturbation calculations, since the validity of a perturbation expansion in strong interaction is very doubtful. In other words, one should study infinite sets of diagrams.

In this paper, we study the infinite-energy behavior of a certain infinite set of diagrams in QED. These are the multiphoton exchange diagrams shown in Fig. 1 for the ee, γe, and $\gamma\gamma$ scattering amplitudes. At infinite s and finite t, the resultant amplitudes of summing these diagrams are all proportional to s, multiplied by simple combinations of eikonal forms. Thus, the eikonal form and the Regge form of high-energy amplitudes can be viewed, respectively, as reflecting the special characteristics of the two different categories of diagrams shown in Figs. 1 and 2. The main results of this paper have been reported in a letter.[5]

It is not the purpose of studying this set of multiphoton exchange diagrams to determine the exact high-energy behavior of amplitudes in QED. The exact high-energy behavior can be found only if all diagrams are analyzed. Such a task seems impossible to accomplish at present. We feel that, for the time being, it is important to associate simple physical features with special sets of diagrams and to develop techniques of calculation before a more realistic description of the true high-energy behavior can be attempted.

The method of calculation in this paper is what we call the "infinite-momentum technique," which exploits the simple Lorentz-transformation properties of the variables $p_\pm\equiv p^0\pm p^3$ and their special properties under the momentum integration.[6] It is also our purpose here to demonstrate in detail how the infinite-momentum technique is used in practical calculations,

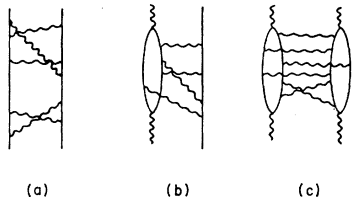

FIG. 1. Multiphoton exchange diagrams: (a) ee scattering; (b) γe scattering; (c) $\gamma\gamma$ scattering. The s channel is always vertical.

* Supported in part by the National Science Foundation. Present address: Department of Physics, University of Illinois, Urbana, Ill.

† On leave of absence from the University of California, San Diego, La Jolla, Calif.

[1] R. J. Glauber, in *Lectures in Theoretical Physics*, edited by W. E. Britten and L. G. Dunham (Wiley-Interscience, Inc., New York, 1959), Vol. 1; T. T. Wu, Phys. Rev. **108**, 466 (1957); R. Torgerson, *ibid.* **143**, 1194 (1966).

[2] T. T. Chou and C. N. Yang, Phys. Rev. **170**, 1591 (1968); **175**, 1832 (1968).

[3] B. W. Lee and R. F. Sawyer, Phys. Rev. **127**, 2266 (1962). See also R. J. Eden *et al.*, *The Analytic S-Matrix* (Cambridge University Press, London, 1966).

[4] H. Cheng and T. T. Wu, Phys. Rev. Letters **22**, 666 (1969); Phys. Rev. **182**, 1852 (1969) (I); **182**, 1868 (1969) (II); **182**, 1873 (1969) (III); **182**, 1899 (1969) (IV).

[5] S. J. Chang and S. Ma, Phys. Rev. Letters **22**, 1334 (1969).

[6] S. J. Chang and S. Ma, Phys. Rev. **180**, 1506 (1969).

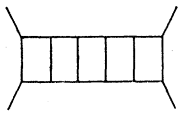

FIG. 2. A t-channel ladder diagram in the scalar-meson model contributing to the Regge behavior.

hoping that this technique will be further developed and applied to various problems by interested readers.

The outline of this paper is the following. In Sec. II, we illustrate the basic aspects of the infinite-momentum technique. Much of the material in this section has been presented in Ref. 6. In Sec. III, we show how the leading s dependence in the high-energy limit can be estimated by inspecting the diagram. To demonstrate further the details of the infinite-momentum technique, we work out in Sec. IV the two-photon exchange diagram in ee scattering and the electron loop integral which appears in later sections. With the technique fully illustrated, the summation of multiphoton exchange diagrams is carried out in Secs. V and VI. In Sec. VII, the results are put into more explicit forms, and the gauge invariance of our procedure is demonstrated. Possible modifications of the results by those diagrams not included are discussed in Sec. VIII. Two short appendices are included to give a few useful formulas and the results of summing the multiphoton exchange diagrams in the charged scalar-meson model.

II. INFINITE-MOMENTUM TECHNIQUE

1. Momentum Variables

We are interested in studying scattering processes in the infinite-energy limit. We must therefore use a set of variables which describes particles moving with infinite momenta in a natural and effective way. The set of variables $(p^0\pm p^3, p^1, p^2)$ studied in Ref. 6 seems to be a reasonable choice. We now proceed to review the basic properties of these variables and list some useful formulas.

Consider a particle moving with an infinitely large momentum. Let the four-momentum be p and let the coordinate axes be chosen in such a way that p^3 is infinite and p^1 and p^2 are finite. Let P be an infinitely large number so that

$$p^3=\eta P \tag{2.1}$$

and η is finite. We then have

$$\begin{aligned} p^0&=[(p^3)^2+\mathbf{p}^2+m^2]^{1/2}\\ &=\eta P+(2\eta P)^{-1}(\mathbf{p}^2+m^2)+O(P^{-3}),\\ \mathbf{p}&=(p^1,p^2). \end{aligned} \tag{2.2}$$

The boldface letters will always denote vectors in the 1, 2 plane.

We shall often refer to the third component of a vector as the *longitudinal* component and the 1, 2 components as the *transverse* components. One can form from p^0 and p^3 the *large* and *small* combinations

$$\begin{aligned} p_+&=p^0+p^3=p_+'(2P)+O(P^{-1}),\\ p_-&=p^0-p^3=p_-'(2P)^{-1}+O(P^{-3}), \end{aligned} \tag{2.3}$$

where

$$p_+'=\eta, \quad p_-'=(\mathbf{p}^2+m^2)/\eta. \tag{2.4}$$

The special decomposition of p into $p_\pm$, $\mathbf{p}$ has a special physical meaning. They are the eigenvectors of the boost operator K_3:

$$i[K_3,p_\pm]=\pm p_\pm, \quad i[K_3,\mathbf{p}]=0. \tag{2.5}$$

Under a Lorentz transformation along the 3 axis, any operator O transforms according to

$$O\rightarrow e^{i\xi K_3}Oe^{-i\xi K_3}.$$

Thus, p transforms accordingly as

$$\mathbf{p}\rightarrow\mathbf{p}, \quad p_\pm\rightarrow e^{\pm\xi}p_\pm. \tag{2.6}$$

Let us choose a *standard Lorentz frame* defined via the Lorentz transformation given by

$$e^\xi=2P. \tag{2.7}$$

Thus, under this Lorentz transformation $p'\rightarrow p$,

$$p_+=(2P)p_+', \quad p_-=(2P)^{-1}p_-', \tag{2.8}$$

and $\mathbf{p}$ is unchanged. This is the same statement as (2.3), of course. The finite vector p' is thus the momentum p measured in the standard frame defined above.

Physically, this standard frame is a reference frame moving with a particle of unit mass which has a momentum P along the third axis. The variables $(p_\pm',\mathbf{p})$ are finite and are very useful in calculations. In all computations involving infinite momenta, we shall always manage to transform to a standard frame. After such a transformation, the momentum variables become finite and the infinite quantities show up as the Lorentz-transformation parameters.

2. Spinors and Polarization Vectors

For computing the scattering amplitudes, we also need to know the transformation laws of the Dirac spinors, photon polarization vectors, and propagators. Let us first work out some of the basic transformation properties of the Dirac spinors. Consider first the simple expression

$$\bar{u}_2(p_2)\gamma^\mu u_1(p_1), \tag{2.9}$$

where the longitudinal components of p_1 and p_2 are infinite, i.e.,

$$p_a{}^3=p_a{}'^3P, \quad P\rightarrow\infty, \quad a=1,2$$

and their transverse components $\mathbf{p}_a'=\mathbf{p}_a$ and $p_a{}'^3$ are finite.

To evaluate (2.9), we perform a Lorentz transformation to the standard frame. The spinors transform according to

$$u(p_1)=e^{-\frac{1}{2}i\xi\sigma^{03}}u(p_1'), \quad \bar{u}(p_2)=\bar{u}(p_2')e^{\frac{1}{2}i\xi\sigma^{03}}, \tag{2.10}$$

where $p_{1,2}'$ are the corresponding four-vectors in the standard frame, $\sigma^{\mu\nu}=\frac{1}{2}i[\gamma^\mu,\gamma^\nu]$, and $e^\xi=2P$. Then (2.9)

reduces to

$$\bar{u}_2(p_2')e^{\frac{1}{2}i\xi\sigma^{03}}\gamma^\mu e^{-\frac{1}{2}i\xi\sigma^{03}}u_1(p_1'). \tag{2.11}$$

The γ matrices transform like the components of a vector, i.e.,

$$e^{\frac{1}{2}i\xi\sigma^{03}}\gamma_\pm e^{-\frac{1}{2}i\xi\sigma^{03}}=e^{\pm\xi}\gamma_\pm, \tag{2.12}$$

and $\boldsymbol{\gamma}$ remains unchanged, where $\gamma_\pm\equiv\gamma^0\pm\gamma^3$ and $\boldsymbol{\gamma}=(\gamma^1,\gamma^2)$. Since $e^\xi=2P\to\infty$, the leading component of (2.11) is $\mu=+$, i.e.,

$$\begin{aligned}\bar{u}_2(p_2)\gamma_+u_1(p_1)&=2P\bar{u}_2(p_2')\gamma_+u_1(p_1')\\&=(2P/m)(p_{1+}'p_{2+}')^{1/2}\delta_{\lambda_1\lambda_2}.\end{aligned} \tag{2.13}$$

The λ's are helicities of the electron. The last step may not be obvious to some readers and is worked out explicitly in Appendix A. It is interesting that the transverse components of p_1 and p_2 do not appear. The lack of spin flip plays an important role in the future computations.

When electron loops are involved in an amplitude, one encounters traces taken over products of γ matrices. To see qualitatively how these traces behave at the infinite-momentum limit, let us work out a simple example.

Consider

$$\mathrm{Tr}[\gamma^\mu(\not{p}_1+m)\gamma^\nu(\not{p}_2+m)], \tag{2.14}$$

where p_1 and p_2, as before, have infinite longitudinal components. After inserting $e^{-\frac{1}{2}i\xi\sigma^{03}}e^{\frac{1}{2}i\xi\sigma^{03}}$ between all pairs of γ matrices, and carrying out the transformation $e^{\frac{1}{2}i\xi\sigma^{03}}\gamma e^{-\frac{1}{2}i\xi\sigma^{03}}$, we find that (2.14) reduces to

$$\mathrm{Tr}\left[\begin{pmatrix}(2P)^{\pm1}\gamma_\pm\\ \boldsymbol{\gamma}\end{pmatrix}(\not{p}_1'+m)\begin{pmatrix}(2P)^{\pm1}\gamma_\pm\\ \boldsymbol{\gamma}\end{pmatrix}(\not{p}_2'+m)\right]. \tag{2.15}$$

This shows that the leading component of the tensor (2.14) is given by $\mu=\nu=+$. This is similar to the fact that the leading component of the vector (2.9) is given by $\mu=+$.

In general, it is possible to transform an arbitrary expression involving Dirac spinors and γ matrices into a corresponding expression in the standard frame covariantly. Any free index μ, as demonstrated above, always picks up a factor $(2P)^{\pm1}$ for $\mu=\pm$.

Similar transformation laws can be obtained for expressions involving photon polarization vectors. The polarization vector $\epsilon_i{}^\mu(p)$ is normalized according to

$$-\epsilon_i{}^\mu(p)\epsilon_{j\mu}(p)=\delta_{ij}, \tag{2.16}$$

where i, j denote the polarizations of the photons and μ is a vector index. Note that the scalar product $A_\mu B^\mu$ is given by $\frac{1}{2}(A_+B_-+A_-B_+)-\mathbf{A}\cdot\mathbf{B}$. The polarization vector has to satisfy the Lorentz condition

$$p_\mu\epsilon_i{}^\mu(p)=0. \tag{2.17}$$

We find that it is advantageous to impose also the radiation gauge condition

$$\bar{p}_\mu\epsilon_i{}^\mu(p)=0, \tag{2.18}$$

where $\bar{p}^0=0$, $\bar{p}^l=p^l$, $l=1, 2, 3$. Obviously, (2.17) and (2.18) imply

$$\epsilon_i{}^0(p)=0 \tag{2.19}$$

and

$$\epsilon_{i\pm}(p)\equiv\epsilon_i{}^0(p)\pm\epsilon_i{}^3(p)=\mp(2P)^{-1}2\mathbf{p}\cdot\boldsymbol{\varepsilon}_i(p). \tag{2.20}$$

It is quite straightforward to transform the polarization vector $\epsilon_i{}^\mu(p)$ into that in the standard frame $\epsilon_i{}'^\mu(p')$ since it transforms covariantly as a four-vector. In the standard frame we have

$$\begin{aligned}&\boldsymbol{\varepsilon}_i'(p')=\boldsymbol{\varepsilon}_i(p),\\&\epsilon_{i+}'(p')=(2P)^{-2}2\mathbf{p}\cdot\boldsymbol{\varepsilon}_i(p)=0,\\&\epsilon_{i-}'(p')=2\mathbf{p}\cdot\boldsymbol{\varepsilon}_i(p),\end{aligned} \tag{2.21}$$

as well as the normalization condition

$$\boldsymbol{\varepsilon}_i'(p')\cdot\boldsymbol{\varepsilon}_j'(p')=\delta_{ij}. \tag{2.22}$$

The fact that $\epsilon_{i+}'(p')=0$ will lead to a tremendous simplification in the evaluation of Compton and the photon-photon scattering amplitudes. This simplification originates from the particular gauge that we have chosen. Of course, other choices of gauges will lead to the same physical result of interest.

We conclude this section by evaluating the propagator

$$[(p+q)^2-m^2+i\epsilon]^{-1}, \tag{2.23}$$

where p has an infinite longitudinal component P. The quantities p^2, $\mathbf{p}$, and q are finite. Factors like (2.23) appear repeatedly in the scattering amplitudes where q, in general, is related to the momentum transfer. In terms of the quantities in the standard frame, we have

$$p_\pm=(2P)^{\pm1}p_\pm', \quad \mathbf{p}=\mathbf{p}'. \tag{2.24}$$

Equation (2.23) becomes

$$\begin{aligned}&[(2Pp_+'+q_+)((2P)^{-1}p_-'+q_-)-(\mathbf{p}+\mathbf{q})^2-m^2+i\epsilon]^{-1}\\&=(2P)^{-1}[p_+'q_-+(2P)^{-1}(p^2+q^2-2\mathbf{p}'\cdot\mathbf{q}-m^2)+i\epsilon]^{-1}\\&=(2P)^{-1}[p_+'q_-+O(P^{-1})+i\epsilon]^{-1}.\end{aligned} \tag{2.25}$$

Equation (2.25) is very useful in later applications.

So far we have restricted our discussion to infinite momenta along the positive 3 direction. It is clear that all that has been said can be applied to infinite momenta along the negative 3 direction by simply interchanging the symbols + and − in appropriate places. In studying scattering at infinite energy, one always encounters infinite and opposite momenta.

III. s DEPENDENCE OF DIAGRAMS

In this section, we shall show how to pick out the leading term in the scattering amplitude for a given diagram as s, the total center-of-mass energy, tends to ∞. The processes we consider here are limited to the two-body elastic scattering $a+b\to a+b$ with a finite momentum transfer. We shall work in the center-of-mass system with the momentum transfer $\mathbf{k}$ lying in the 1, 2 plane. The kinematics is shown in Fig. 3. The

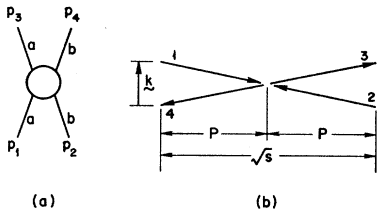

FIG. 3. Kinematics of $a+b \to a+b$.

initial and final momenta are conveniently expressed in terms of the purely longitudinal momenta p_a, p_b and the purely transverse momentum transfer k:

$$\begin{aligned} p_1 &= p_a - \tfrac{1}{2}k, \quad p_2 = p_b + \tfrac{1}{2}k, \\ p_3 &= p_a + \tfrac{1}{2}k, \quad p_4 = p_b - \tfrac{1}{2}k, \end{aligned} \tag{3.1}$$

where

$$p_a{}^3 = -p_b{}^3 = P, \quad \mathbf{p}_{a,b} = 0, \quad k^3 = 0. \tag{3.2}$$

The total energy squared of the system is

$$\begin{aligned} s &= (p_1+p_2)^2 \\ &= [(m_a{}^2 + \tfrac{1}{4}\mathbf{k}^2 + P^2)^{1/2} + (m_b{}^2 + \tfrac{1}{4}\mathbf{k}^2 + P^2)^{1/2}]^2 \\ &= (2P)^2 + O(1). \end{aligned} \tag{3.3}$$

In terms of components $p = (p_+, p_-, \mathbf{p})$, (3.1) becomes, owing to (3.2) and (3.3),

$$\begin{aligned} p_1 &= (s^{1/2}, s^{-1/2}(\tfrac{1}{4}\mathbf{k}^2 + m_a{}^2), -\tfrac{1}{2}\mathbf{k}), \\ p_3 &= (s^{1/2}, s^{-1/2}(\tfrac{1}{4}\mathbf{k}^2 + m_a{}^2), \tfrac{1}{2}\mathbf{k}), \\ p_2 &= (s^{-1/2}(\tfrac{1}{4}\mathbf{k}^2 + m_b{}^2), s^{1/2}, \tfrac{1}{2}\mathbf{k}), \\ p_4 &= (s^{-1/2}(\tfrac{1}{4}\mathbf{k}^2 + m_b{}^2), s^{1/2}, -\tfrac{1}{2}\mathbf{k}). \end{aligned} \tag{3.4}$$

To facilitate our discussion, we shall use the symbol p to replace the word "momentum" in various contexts. For example, instead of saying that "the electron has a momentum whose + component is infinite and whose − component is infinitesimal," we simply say that "the electron has an infinite p_+ and an infinitesimal p_-."

Thus, according to (3.4) the external lines 1, 3 have infinite p_+ and 2, 4 have infinite p_-, as $s \to \infty$. Since the momentum is conserved at each vertex, the infinite p_+ and p_- must be carried through some of the internal lines. As far as the leading terms are concerned, we find the following general rule: *No internal line can carry both an infinite p_+ and an infinite p_- simultaneously as $s \to \infty$.* The reason goes roughly as follows.

The invariant p^2 of an internal line goes like p_+p_-, which tends to ∞ if both p_+ and p_- do. Since p^2 occurs in the denominator of the propagator, the internal line with infinite p_+ and infinite p_- tends to diminish the amplitude. Therefore, the leading contribution must come from graphs with no internal lines carrying infinite p_+ and p_- simultaneously. We have verified this rule for simple diagrams although we have not proved it in general. At present, we shall take it as a working rule for estimating the s dependence of a diagram.

To see how our method is useful in practice, let us consider some lowest-order electron-position scattering amplitudes, (see Fig. 4). It is easy to see that the internal photon line in diagram 4(a) carries both an infinite p_+ and an infinite p_- as $s \to \infty$, while the photon line in diagram 4(b) carries only a finite momentum. According to the above rule, we should expect that the contribution from diagram 4(a) is small in comparison with that from diagram 4(b) as $s \to \infty$. Let us verify this explicitly. For diagram 4(a), the amplitude, i.e., *the invariant T-matrix element*, is

$$\begin{aligned} -\bar{u}(p_a+\tfrac{1}{2}k)\gamma^\mu v(p_b-\tfrac{1}{2}k)\bar{v}(p_b+\tfrac{1}{2}k)\gamma_\mu u(p_a-\tfrac{1}{2}k) \\ \times[(p_a+p_b)^2 - \mu^2 + i\epsilon]^{-1}, \end{aligned} \tag{3.5}$$

where μ is a fictious photon mass which is included to remove the posible infrared divergence.

Let us introduce two standard frames a and b, a for the spinors with infinite p_+ and b for those with infinite p_-.

The spinors with infinite p_+ are related to the spinors in the standard frame a through

$$\begin{aligned} u(p_a - \tfrac{1}{2}k) &= e^{-\frac{1}{2}i\xi\sigma^{03}} u(p_a{}' - \tfrac{1}{2}k), \\ \bar{u}(p_a + \tfrac{1}{2}k) &= \bar{u}(p_a{}' + \tfrac{1}{2}k) e^{\frac{1}{2}i\xi\sigma^{03}}, \end{aligned} \tag{3.6}$$

$$p_{a+}{}' = 1. \tag{3.7}$$

For the spinors with infinite p_-, i.e., the v and $\bar{v}$ in (3.5), expressions similar to (3.6) can be written down with $p_{b-}{}' = 1$ in the standard frame b. The photon propagator has infinite p_+ and p_-. It simply gives $1/s$ as $s \to \infty$. In terms of spinors in the standard frames, (3.5) reduces to

$$\begin{aligned} -\bar{u}(p_a{}' + \tfrac{1}{2}k) e^{\frac{1}{2}i\xi\sigma^{03}} \gamma^\mu e^{\frac{1}{2}i\xi\sigma^{03}} v(p_b{}' - \tfrac{1}{2}k) \bar{v}(p_b{}' + \tfrac{1}{2}k) \\ \times e^{-\frac{1}{2}i\xi\sigma^{03}} \gamma_\mu e^{-\frac{1}{2}i\xi\sigma^{03}} u(p_a{}' - \tfrac{1}{2}k)(1/s). \end{aligned} \tag{3.8}$$

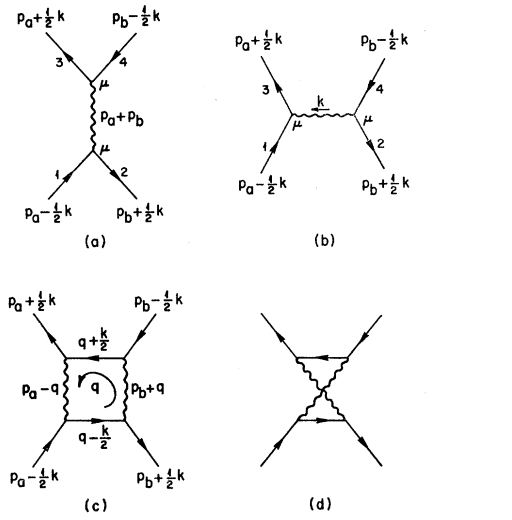

FIG. 4. (a) An e^+e^- scattering diagram not contributing to the leading term. (b) A diagram contributing to the leading term. (c) and (d) Two-photon exchange e^+e^- diagrams not contributing to the leading term.

It is easy to verify that $\gamma_\pm$ anticommute and γ commutes with σ^{03}. Therefore, for the terms with $\mu=\pm$ in (3.8), the exponential factors cancel as we move $\gamma_\pm$ to the right or to the left. The result is of $O(1/s)$. For $\mu=1, 2$, the exponential factors combine and give

$$e^{i\xi\sigma^{03}} \to \tfrac{1}{2}(\sqrt{s})(1+i\sigma^{03}) \tag{3.9}$$

and the resultant amplitude is of $O(1)$.

For diagram 4(b), there is no additional damping factor in the denominator, and the amplitude is given by

$$\bar{u}_3(p_a+\tfrac{1}{2}k)\gamma^\mu u_1(p_a-\tfrac{1}{2}k)\bar{v}_2(p_b+\tfrac{1}{2}k)\gamma_\mu v_4(p_b-\tfrac{1}{2}k) \times(k^2-\mu^2+i\epsilon)^{-1}. \tag{3.10}$$

In terms of the variables in the standard frames and with the help of (2.13), the leading term in (3.10) as $s\to\infty$ is the term with $\mu=+$ in the first factor coupled with $\mu=-$ in the second factor, giving

$$s\bar{u}_3(p_a'+\tfrac{1}{2}k)\gamma_+u_1(p_a'-\tfrac{1}{2}k)\bar{v}_2(p_b'+\tfrac{1}{2}k) \times\gamma_-v_4(p_b'-\tfrac{1}{2}k)(k^2-\mu^2+i\epsilon)^{-1} = -sm^{-2}\delta_{\lambda_1\lambda_3}\delta_{\lambda_2\lambda_4}(k^2-\mu^2+i\epsilon)^{-1}. \tag{3.11}$$

Notice that when u is replaced by v in (2.13), a minus sign on the right-hand side is needed. Indeed, (3.11) is an order of s larger than the contribution of diagram 4(a). Note that the leading contribution in diagram 4(b) is due to the coupling via the photon between the large component of $\bar{u}\gamma^\mu u$ on the left ($\mu=+$) to the large component of $\bar{v}\gamma^\mu v$ on the right ($\mu=-$), which are associated with the electron and positron of large and opposite momenta. The coupling between these large components is possible because photon has spin 1. This very property plays an important role in the high-energy asymptotic behavior of all QED scattering amplitudes.

Next, let us consider the e^+e^- elastic scattering amplitudes with two photons exchanged. According to our rule, it is very easy to see that diagram 4(d) cannot be the leading term because at least one of its internal lines must carry an infinite p_+ and an infinite p_- simultaneously. Diagram 4(c) is a little tricky. None of the internal lines carry both infinite p_+ and infinite p_- for finite q. However, as we shall see, this diagram still cannot give a leading s dependence because the particles exchanged between the fast-moving particles are electrons rather than photons. In fact, the larger the spin of the particle exchanged, the higher the leading power in s in the final amplitude. To see this, let us work out explicitly the contribution from Fig. 4(c).

The amplitude is

$$\int\frac{d^4q}{i(2\pi)^4}\bar{u}(p_a+\tfrac{1}{2}k)\gamma^\mu(\boldsymbol{q}-\tfrac{1}{2}\boldsymbol{k}+m)\gamma^\nu v(p_b-\tfrac{1}{2}k)\bar{v}(p_b+\tfrac{1}{2}k)\gamma_\nu(\boldsymbol{q}+\tfrac{1}{2}\boldsymbol{k}+m)\gamma_\mu u(p_a-\tfrac{1}{2}k)[(p_a-q)^2-\mu^2+i\epsilon]^{-1} \times[(p_b+q)^2-\mu^2+i\epsilon]^{-1}[(q-\tfrac{1}{2}k)^2-m^2+i\epsilon]^{-1}[(q+\tfrac{1}{2}k)^2-m^2+i\epsilon]^{-1}$$

$$=\int\frac{d^4q}{i(2\pi)^4}\bar{u}(p_a'+\tfrac{1}{2}k)\gamma^\mu e^{\frac{1}{2}i\xi\sigma^{03}}(\boldsymbol{q}-\tfrac{1}{2}\boldsymbol{k}+m)e^{\frac{1}{2}i\xi\sigma^{03}}\gamma^\nu v(p_b'-\tfrac{1}{2}k)\bar{v}(p_b'+\tfrac{1}{2}k)\gamma_\nu e^{-\frac{1}{2}i\xi\sigma^{03}}(\boldsymbol{q}+\tfrac{1}{2}\boldsymbol{k}+m)e^{-\frac{1}{2}i\xi\sigma^{03}}\gamma_\mu u(p_a'-\tfrac{1}{2}k) \times[(\sqrt{s})(-q_-+O(1/\sqrt{s})+i\epsilon)]^{-1}[(\sqrt{s})(q_++O(1/\sqrt{s})+i\epsilon)]^{-1} \times[(q-\tfrac{1}{2}k)^2-m^2+i\epsilon]^{-1}[(q+\tfrac{1}{2}k)^2-m^2+i\epsilon]^{-1}, \tag{3.12}$$

where we have made use of (2.25) and (3.6). Analogous to the amplitude in Fig. 4(a), the numerator goes like s, and consequently the amplitude goes as $O(1)$. In other words, the leading s dependence generated in the numerators of an amplitude associated with an e^+e^- pair-exchanged is overcompensated by the $1/s$ factors picked up from the denominators. One can verify for the lowest-order diagrams that this is also a general result. In the future, we consider only processes with an arbitrary number of photons being exchanged between particles carrying large and opposite momenta.

In the above calculations, we have assumed that we can factor out the s dependence before the loop integration is carried out. In the present case and that of the two-photon exchange amplitude, the validity of the factorization (up to $\ln s$) can be established. In general, it is certainly of great importance to give a simple criterion and justification for factoring out the s dependence. The criterion we use in our calculations is simply that the remaining integral after the leading s dependence has been factored out should be finite and well behaved. When any term, even if it is an order or so smaller in s in appearance, becomes divergent after s factors have been taken out, we must keep this term in its original form and perform the integral first. In general, this latter integral becomes convergent and there appears a cutoff of order s to the integral. We then factor out the s dependence after the integration if the remaining coefficient is then finite. In other words, we make sure that the remaining integrals are finite when we factor out the s dependence.

IV. PROCESSES WITH TWO-PHOTON EXCHANGE

In this section, we consider the asymptotic amplitudes for processes with two-photon exchange. These diagrams have been studied thoroughly by Cheng and Wu.[4] We

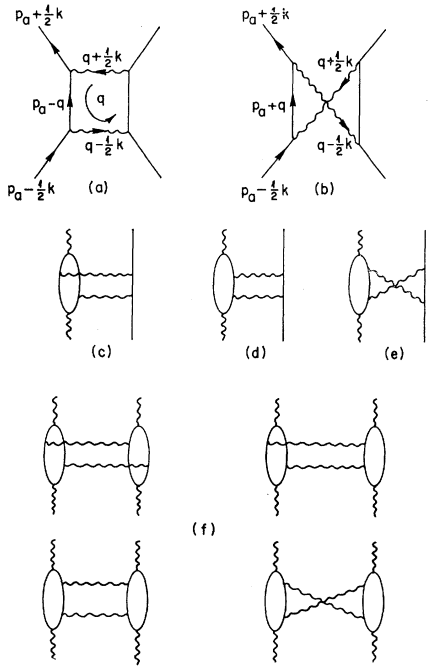

FIG. 5. (a) and (b) Leading two-photon exchange ee scattering diagrams. (c)–(f) Lowest-order leading γe and $\gamma\gamma$ scattering diagrams.

wish to use these relatively simple diagrams to demonstrate our technique.

We first consider the ee scattering amplitude given in Figs. 5(a) and 5(b). The amplitude for diagram 5(a) is

$$-e^4\int\frac{d^4q}{i(2\pi)^4}\times\frac{A^{\mu\nu}B_{\mu\nu}}{[(q+\frac{1}{2}k)^2-\mu^2+i\epsilon][(q-\frac{1}{2}k)^2-\mu^2+i\epsilon]}, \quad (4.1)$$

where

$$A^{\mu\nu}=\bar{u}_3(p_a+\tfrac{1}{2}k)\gamma^\mu(\not{p}_a-\not{q}+m)\gamma^\nu u_1(p_a-\tfrac{1}{2}k)\times[(p_a-q)^2-m^2+i\epsilon]^{-1}, \quad (4.2)$$

$$B_{\mu\nu}=\bar{u}_4(p_b-\tfrac{1}{2}k)\gamma_\mu(\not{p}_b+\not{q}+m)\gamma_\nu u_2(p_b+\tfrac{1}{2}k)\times[(p_b+q)^2-m^2+i\epsilon]^{-1}. \quad (4.3)$$

As always, the amplitude is evaluated in the c.m. frame with k lying in the 1, 2 plane. To compute the leading behavior in s, we factor out the s dependence before the loop integration. We have mentioned at the end of the last section that one has to be very careful about the interchange of the limit $s\to\infty$ and the loop integration. The validity of our procedure may be justified afterwards by showing that the resulting coefficient of the s factor is finite and well behaved. Note that for a fixed q, we can compute the asymptotic behavior of $A^{\mu\nu}$ and $B^{\mu\nu}$ separately, and put them back into (4.1) after the s dependences are factored out.

Let us first compute the asymptotic s dependence of $A_{\mu\nu}$. We follow the method outlined in Sec. II, and express $A^{\mu\nu}$ in terms of quantities in the standard frame. The transformation property of $A^{\mu\nu}$ is very simple. The leading component of $A^{\mu\nu}$ is $\mu=\nu=+$, giving

$$A_{++}=(\sqrt{s})\bar{u}_3(p_a'+\tfrac{1}{2}k)\gamma_+(\not{p}_a'-\not{q}'+m)\gamma_+u_1(p_a'-\tfrac{1}{2}k)\times[-q_-+O(q^2/\sqrt{s})+i\epsilon]^{-1}, \quad (4.4)$$

where

$$q_\pm'=s^{\mp1/2}q_\pm, \quad \mathbf{q}'=\mathbf{q}.$$

Since

$$\gamma_+^2=\gamma_+\gamma\gamma_+=0, \quad \gamma_+\gamma_-\gamma_+=4\gamma_+,$$

only γ_- can survive between the two γ_+'s, and consequently,

$$\gamma_+(\not{p}_a'-\not{q}'+m)\gamma_+=2(p_a'+q')_+\gamma_+=2\gamma_+.$$

Then, with the help of (2.13), Eq. (4.4) reduces to

$$A_{++}=2[(\sqrt{s})/m]\delta_{\lambda_1\lambda_3}[-q_-+O(q^2/\sqrt{s})+i\epsilon]^{-1}, \quad (4.5)$$

where $\delta_{\lambda_1\lambda_3}$ indicates that the helicity of the electron does not flip. Similarly, the asymptotic structure of $B_{\mu\nu}$ can be obtained as

$$B_{--}=2[(\sqrt{s})/m]\delta_{\lambda_2\lambda_4}[q_+-O(q^2/\sqrt{s})+i\epsilon]^{-1}. \quad (4.6)$$

Substituting (4.5) and (4.6) back into (4.1), we have

$$A^{\mu\nu}B_{\mu\nu}=\tfrac{1}{4}A_{++}B_{--}+O(1),$$

and the asymptotic amplitude for diagram 5(a) is

$$-\tfrac{1}{2}e^4sm^{-2}\delta_{\lambda_1\lambda_3}\delta_{\lambda_2\lambda_4}\int\frac{dq_+dq_-d^2q}{i(2\pi)^4}[-q_-+O(q^2/\sqrt{s})+i\epsilon]^{-1}\times[q_+-O(q^2/\sqrt{s})+i\epsilon]^{-1}[(q+\tfrac{1}{2}k)^2-\mu^2+i\epsilon]^{-1}\times[(q-\tfrac{1}{2}k)^2-\mu^2+i\epsilon]^{-1}. \quad (4.7)$$

Diagram 5(b) leads to the same contribution as that of diagram 5(a), except that the q in (4.5) is changed to $-q$ [or, alternatively, the q in (4.6) is changed to $-q$]. Adding the two diagrams, and ignoring the $O(q^2/\sqrt{s})$ terms, we find that a factor

$$(-q_-+i\epsilon)^{-1}+(q_-+i\epsilon)^{-1}=-2\pi i\delta(q_-) \quad (4.8)$$

results in A_{++}. Similarly, by averaging over q and $-q$ in the denominator of B_{--}, we have

$$B_{--}\to(\sqrt{s})\delta_{\lambda_2\lambda_4}(-2\pi i)\delta(q_+). \quad (4.9)$$

Collecting terms and performing the loop integrals in (4.7), we have the fourth-order e^-e^- (or e^-e^+) scattering amplitude

$$-\tfrac{1}{4}ism^{-2}\delta_{\lambda_1\lambda_3}\delta_{\lambda_2\lambda_4}e^4\times\int d^2q(2\pi)^{-2}[(\mathbf{q}+\tfrac{1}{2}\mathbf{k})^2+\mu^2]^{-1}[(\mathbf{q}-\tfrac{1}{2}\mathbf{k})^2+\mu^2]^{-1}=\tfrac{1}{2}is\delta_{\lambda_1\lambda_3}\delta_{\lambda_2\lambda_4}m^{-2}\left[-\frac{1}{2}\int d^2b\, e^{i\mathbf{k}\cdot\mathbf{b}}\chi(\mathbf{b})^2\right], \quad (4.10)$$

with

$$\chi(\mathbf{b})=-e^2\int d^2q(2\pi)^{-2}(\mathbf{q}^2+\mu^2)^{-1}e^{i\mathbf{q}\cdot\mathbf{b}}. \quad (4.11)$$

There are two important features illustrated above. First, only γ_+ appears at the vertices on the electron line on the left, and only γ_- on the right. Second, as a result of adding the diagrams in Figs. 5(a) and 5(b), $\delta(q_\pm)$ appear. As we shall see, both features persist when additional photons are exchanged between the electrons.

For each of the individual diagrams, such as Fig. 5(a), the result is less appealing. For example, we cannot ignore the $O(q^2/\sqrt{s})$ terms in the denominator of (4.7) without making the $q_\pm$ integrals diverge logarithmically. This indicates that these $O(q^2/\sqrt{s})$ terms must serve as cutoffs on the loop integrations. Indeed, if one keeps these $1/\sqrt{s}$ terms, the $q_\pm$ integrals become convergent and the amplitude (4.7) behaves asymptotically as

$$\sim -s\ln s\frac{\delta_{\lambda_1\lambda_3}\delta_{\lambda_2\lambda_4}}{2\pi}\int\frac{d^2q}{(2\pi)^2}[(\mathbf{q}+\tfrac{1}{2}\mathbf{k})^2+\mu^2-i\epsilon]^{-1}\times[(\mathbf{q}-\tfrac{1}{2}\mathbf{k})^2+\mu^2-i\epsilon]^{-1}. \quad (4.12)$$

It is important to recognize that the $\ln s$ factor in (4.12) is due to the nonvanishing principal parts of the denominators

$$[-q_-+O(q^2/\sqrt{s})+i\epsilon]^{-1}[q_++O(q^2/\sqrt{s})+i\epsilon]^{-1}. \quad (4.13)$$

When all crossed diagrams of a given order are added together, the principal parts cancel and so do all the $s\ln s$ terms.

The requirement of gauge invariance gives a fundamental reason why one is only interested in the total amplitude in which all crossed diagrams of a given order are included. The individual diagram, such as Fig. 5(a), by itself is not gauge-invariant. We have to add up diagrams of all possible crossed photon lines in order to make the final result gauge-invariant. The appearance of $s\ln s$ in (4.7) is a reflection of the non-gauge-invariant nature of the amplitude. This point will be discussed in more detail in Sec. VII.

We now proceed to evaluate the γe and $\gamma\gamma$ amplitude given in Figs. 5(c)–5(f). All these amplitudes can be expressed in the form (4.1) with $A_{\mu\nu}$ (and $B_{\mu\nu}$) depending on the particular type of incident particles. For the photon subdiagrams in Figs. 6(a)–6(c), the amplitudes for $A_{\mu\nu}$ are, respectively,

$$A_{ij}{}^{(a)\mu\nu}=-\int\frac{d^4w}{i(2\pi)^4}M_{ij}{}^{\mu\nu}(-q+\tfrac{1}{2}k,\ q+\tfrac{1}{2}k;\ w)$$

$$=-\int\frac{d^4w}{i(2\pi)^4}\epsilon_\beta{}^j\epsilon_\alpha{}^i\,\mathrm{Tr}[S_F(w-p)\gamma^\alpha S_F(w-\tfrac{1}{2}k)\gamma^\mu\times S_F(w-q)\gamma^\beta S_F(w-q-p-\tfrac{1}{2}k)\gamma^\nu], \quad (4.14)$$

$$A_{ij}{}^{(b)\mu\nu}=-\int\frac{d^4w}{i(2\pi)^4}\epsilon_\beta{}^j\epsilon_\alpha{}^i\,\mathrm{Tr}[S_F(w-p)\gamma^\alpha S_F(w-\tfrac{1}{2}k)\gamma^\mu\times S_F(w-q)\gamma^\nu S_F(w+\tfrac{1}{2}k)\gamma^\beta], \quad (4.15)$$

and

$$A_{ij}{}^{(c)\mu\nu}=A_{ij}{}^{(b)\mu\nu}(q\to -q), \quad (4.16)$$

where

$$S_F(p)=(\not{p}-m+i\epsilon)^{-1}=(\not{p}+m)(p^2-m^2+i\epsilon)^{-1}.$$

The leading components in these A's are those components with $\mu=\nu=+$. We denote these quantities by A_{ij} for simplicity. Let us concentrate on $A_{ij}{}^{(a)}$.

First, consider the propagators 3 and 4, i.e., the two upper propagators. They give rise to two denominators,

$$(w-q)^2-m^2+i\epsilon=(w-q)_+(w-q)_- -(\mathbf{w}-\mathbf{q})^2-m^2+i\epsilon \quad (4.17)$$

and

$$(w-q-p-\tfrac{1}{2}k)^2-m^2+i\epsilon=(w-q-p)_+(w-q-p)_- -(\mathbf{w}-\mathbf{q}-\tfrac{1}{2}\mathbf{k})^2-m^2+i\epsilon. \quad (4.18)$$

In terms of the variables in the standard frame and using $p_+{}'=1$, $p_-{}'=\frac{1}{4}\mathbf{k}^2$, $k_\pm=0$, they become, respectively,

$$-(\sqrt{s})w_+{}'D,$$
$$D\equiv q_-+[(\sqrt{s})w_+{}']^{-1}[(\mathbf{w}-\mathbf{q})^2+m^2-i\epsilon -w_+{}'w_-{}'-q_+q_-]+O(s^{-1}) \quad (4.19)$$

and

$$-(\sqrt{s})(w_+{}'-1)D',$$
$$D'\equiv q_-+[(\sqrt{s})(w_+{}'-1)]^{-1}[(\mathbf{w}-\mathbf{q}-\tfrac{1}{2}\mathbf{k})^2+m^2-i\epsilon-q_+q_- +(1-w_+{}')(w_-{}'-\tfrac{1}{4}\mathbf{k}^2)]+O(s^{-1}). \quad (4.20)$$

The product of these denominators appears to contribute an $O(s^{-1})$ factor. However, it actually contributes an $O(s^{-1/2})$ factor. One must be careful because, if one lets s become infinite directly in (4.19) and in (4.20), one would have, for $0<w_+{}'<1$,

$$(DD')^{-1}=(q_-+i\epsilon)^{-1}(q_--i\epsilon)^{-1}. \quad (4.21)$$

Then, the remaining w' integrals would diverge quadratically and the q_- integral would not be defined either. To do it correctly, we write

$$(DD')^{-1}=(D^{-1}-D'^{-1})(D'-D)^{-1}. \quad (4.22)$$

From (4.19) and (4.20), we see that $D'-D=O(s^{-1/2})$. For $0<w_+{}'<1$, we have

$$D^{-1}-D'^{-1}=(q_--i\epsilon)^{-1}-(q_-+i\epsilon)^{-1} =2\pi i\delta(q_-) \quad (4.23)$$

as $s\to\infty$. Thus, (4.17) and (4.18) contributes an $O(s^{-1/2})$ factor.

The remaining denominators of the propagators 1 and 2 and $D'-D$ can be written as

$$[(w_+{}'-1)(w_-{}'-\tfrac{1}{4}\mathbf{k}^2)-\mathbf{w}^2-m^2+i\epsilon] \times[w_+{}'w_-{}'-(\mathbf{w}-\tfrac{1}{2}\mathbf{k})^2-m^2+i\epsilon] \times s^{-1/2}\{(1-w_+{}')^{-1}[q_+q_--(\mathbf{w}-\mathbf{q}-\tfrac{1}{2}\mathbf{k})^2-m^2+i\epsilon] +\tfrac{1}{4}\mathbf{k}^2+w_+{}'^{-1}[q_+q_--(\mathbf{w}-\mathbf{q})^2-m^2+i\epsilon]\}. \quad (4.24)$$

Note that there is no w_-' dependence in the last denominator. In fact, nor is there any in the numerator of (4.14). The w_-' integration can now be carried out easily. After the w_-' integral, the four denominators 1, 2, 3, and 4 give

$$s^{-1/2}(2\pi i)^2\delta(q_-)[(\mathbf{w}-\mathbf{q}-\tfrac{1}{2}w_+'\mathbf{k})^2+m^2]^{-1} \times\{[\mathbf{w}-\tfrac{1}{2}(1-w_+')\mathbf{k}]^2+m^2\}^{-1} \quad (4.25)$$

for $0<w_+'<1$ and zero otherwise. The finite range in the remaining w_+' integration is a special feature of the infinite-momentum technique. Interested readers are referred to Ref. 6 for more details.

The two denominators in (4.25) can now be combined by introducing the Feynman parameter x. Equation (4.25) becomes

$$s^{-1/2}(2\pi i)^2\delta(q_-)\int_0^1 dx\,[\mathbf{w}''^2+m^2 +x(1-x)(\mathbf{q}+(\beta'-\tfrac{1}{2})\mathbf{k})^2]^{-2}, \quad (4.26)$$

where

$$\mathbf{w}''\equiv\mathbf{w}-\tfrac{1}{2}\beta x\mathbf{k}-(1-x)(\mathbf{q}+\tfrac{1}{2}\beta'\mathbf{k}). \quad (4.27)$$

We have written β' for w_+' and β for $1-w_+'$.

The leading term in the numerator of the integrand in (4.14) can be extracted in the same way as was illustrated previously. We simply give the result of taking the trace:

$$\begin{aligned}8s\{&-k^ik^j(\beta\beta')^2-\beta\beta'(w_2{}^iw_4{}^j+w_4{}^iw_2{}^j+w_1{}^iw_3{}^j+w_3{}^iw_1{}^j)\\&+\beta^2(w_2{}^iw_3{}^j-w_3{}^iw_2{}^j)+\beta'^2(w_1{}^iw_4{}^j-w_4{}^iw_1{}^j)\\&+\beta\beta'(-\beta k^iw_2{}^i+\beta' k^iw_1{}^i-\beta' k^iw_4{}^j+\beta k^iw_3{}^j)\\&+\delta_{ij}[\beta\beta'(\mathbf{w}_2\cdot\mathbf{w}_4+\mathbf{w}_1\cdot\mathbf{w}_3+2m^2)\\&+\beta^2(\mathbf{w}_2\cdot\mathbf{w}_3+m^2)+\beta'^2(\mathbf{w}_1\cdot\mathbf{w}_4+m^2)]\}. \quad (4.28)\end{aligned}$$

The subscripts 1, 2, 3, and 4 refer to the propagator labels in Fig. 6(a) and $w^i=\boldsymbol{\epsilon}^i\cdot\mathbf{w}$. In terms of $\mathbf{w}''$, defined by (4.27) and

$$\mathbf{K}\equiv\beta'(\mathbf{q}+\tfrac{1}{2}\mathbf{k})-\beta(-\mathbf{q}+\tfrac{1}{2}\mathbf{k}), \quad (4.29)$$

(4.28) becomes

$$\begin{aligned}8s\{&4\beta\beta' x(1-x)K^iK^j\\&+\delta_{ij}[(1-2\beta\beta')\mathbf{w}''^2+m^2-x(1-x)\mathbf{K}^2]\}. \quad (4.30)\end{aligned}$$

We have ignored terms linear in $\mathbf{w}''$, since they will not contribute to the $\mathbf{w}''$ integral.

The w integral in (4.14) may be written as

$$\begin{aligned}\int d^4w&=\frac{1}{2}\int dw_+'dw_-'d^2w'\\&=\frac{1}{2}\int_0^1 d\beta d\beta'\delta(1-\beta-\beta')d^2w''dw_-'. \quad (4.31)\end{aligned}$$

The w_-' integration has already been done. Combining

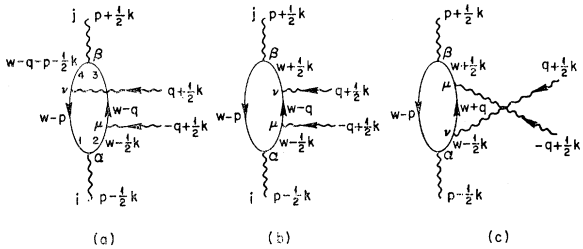

FIG. 6. Left side of Figs. 5(c)–5(f).

(4.30) and (4.26), we have

$$\begin{aligned}e^2A_{ij}{}^{(a)}&=e^2i(2\pi)^{-4}\int d^4w\,M_{ij}(-q+\tfrac{1}{2}k,\,q+\tfrac{1}{2}k;\,w)\\&=-4\pi i(\sqrt{s})\\&\quad\times[I_{ij}(-\mathbf{q}+\tfrac{1}{2}\mathbf{k},\,\mathbf{q}+\tfrac{1}{2}\mathbf{k})+C\delta_{ij}]\delta(q_-), \quad (4.32)\end{aligned}$$

where $\alpha=e^2/4\pi$ is included in the definition of I_{ij} for convenience,

$$\begin{aligned}I_{ij}(\mathbf{k}_1,\mathbf{k}_2)\equiv&\frac{\alpha}{\pi}\int_0^1 d\beta d\beta' dx\delta(1-\beta-\beta')\\&\times[4K^iK^j\beta\beta' x(1-x)-\tfrac{1}{2}\delta_{ij}\mathbf{K}^2(1-8\beta\beta'(x-\tfrac{1}{2})^2)]\\&\times[m^2+x(1-x)\mathbf{K}^2]^{-1}, \quad (4.33)\end{aligned}$$

$$\mathbf{K}\equiv\beta'\mathbf{k}_2-\beta\mathbf{k}_1, \quad (4.34)$$

and C is a logarithmically divergent constant. As we shall see, this logarithmic divergent constant will be canceled out by a similar divergent integral in amplitudes $A_{\mu\nu}{}^{(b)}$ and $A_{\mu\nu}{}^{(c)}$.

Now let us consider the leading components $\mu=\nu=+$ in Figs. 6(b) and 6(c). In terms of variables in the standard frame and after factoring out the s dependence explicitly, we have

$$A_{ij}{}^{(b)}=-\tfrac{1}{2}(\sqrt{s})\times\int\frac{dw_+'dw_-'d^2w}{i(2\pi)^4}\epsilon_{i\alpha}'\epsilon_{j\beta}'\,\mathrm{Tr}[\cdots]D^{-1}, \quad (4.35)$$

where

$$\begin{aligned}D=&[(w_+'-1)(w_-'-\tfrac{1}{4}\mathbf{k}^2)-\mathbf{w}^2-m^2+i\epsilon]\\&\times[w_+'w_-'-(\mathbf{w}-\tfrac{1}{2}\mathbf{k})^2-m^2+i\epsilon]\\&\times[w_+'w_-'-(\mathbf{w}+\tfrac{1}{2}\mathbf{k})^2-m^2+i\epsilon]\\&\times[-w_+'q_-+O(q^2/\sqrt{s})+i\epsilon] \quad (4.36)\end{aligned}$$

and

$$\begin{aligned}\mathrm{Tr}[\cdots]=&\,\mathrm{Tr}[(\boldsymbol{w}'-\boldsymbol{p}'+m)\gamma^\alpha(\boldsymbol{w}'-\tfrac{1}{2}\boldsymbol{k}+m)\gamma_+\\&\times(\boldsymbol{w}'-\boldsymbol{q}'+m)\gamma_+(\boldsymbol{w}'+\tfrac{1}{2}\boldsymbol{k}+m)\gamma^\beta]\\=&\,2w_+'\,\mathrm{Tr}[(\boldsymbol{w}'-\boldsymbol{p}'+m)\gamma^\alpha(\boldsymbol{w}'-\tfrac{1}{2}\boldsymbol{k}+m)\gamma_+\\&\times(\boldsymbol{w}'+\tfrac{1}{2}\boldsymbol{k}+m)\gamma^\beta]. \quad (4.37)\end{aligned}$$

In deriving (4.37), we have used the relation

$$\gamma_+(\boldsymbol{w}'-\boldsymbol{q}'+m)\gamma_+=2(w'-q')_+\gamma_+=2w_+'\gamma_++O(s^{-1/2}).$$

Making use of (2.21) and (2.22), we find that the trace reduces further to

$$\begin{aligned}&\epsilon_i'\epsilon_j'\ \mathrm{Tr}[\cdots]\\&=8w_+'\{k_ik_jw_+'(1-w_+')^2+(1-2w_+'+2w_+'^2)\\&\quad\times(w_jk_i-k_jw_i)-4w_+'w_iw_j+\delta_{ij}[(\tfrac{1}{4}\mathbf{k}^2-w_-')w_+'^2\\&\qquad+w_+'(\mathbf{w}^2+\tfrac{1}{4}\mathbf{k}^2+m^2)+\mathbf{w}^2-\tfrac{1}{4}\mathbf{k}^2+m^2]\}.\end{aligned}\tag{4.38}$$

The expression for $A_{ij}{}^{(c)}$ is identical to that of $A_{ij}{}^{(b)}$ except that the last factor in D is replaced by $w_+'q_-+O(q^2/\sqrt{s})+i\epsilon$. As in the case of *ee* scattering, the q_- integral diverges logarithmically for each of the individual A_{ij}. However, by adding the two diagrams, the last factors in D of these two denominators combine:

$$\frac{1}{-w_+'q_-+i\epsilon}+\frac{1}{w_+'q_-+i\epsilon}=\frac{-2\pi i}{|w_+|}\delta(q_-),\tag{4.39}$$

and the q_- integral becomes trivial.

We next carry out the w' integration. Since there are three w_-' in the denominator D and at most one in the numerator, the w_-' integral always converges. We can close the contour of w_-' integral at $|w_-'|=\infty$ from either above or below the real axis, whichever is more convenient. Note that two of the poles in the w_-' plane are always on the same side of the real axis, and if the third pole is also on the same side of the real axis, the w_-' integral vanishes identically. We then find that the w_-' integral vanishes except for $0<w_+'<1$, and in the later case, the denominator reduces under the w_-' integration to

$$\begin{aligned}D^{-1}=[-(2\pi i)^2\beta/w_+']\delta(q_-)[(\mathbf{w}+\tfrac{1}{2}\beta\mathbf{k})^2+m^2]^{-1}\\\times[(\mathbf{w}-\tfrac{1}{2}\beta\mathbf{k})^2+m^2]^{-1},\end{aligned}\tag{4.40}$$

where $\beta=1-w_+'$. The last two factors in (4.40) can be combined by means of a Feynman parameter x as

$$\int_0^1 dx\,[(\mathbf{w}-\tfrac{1}{2}\beta\mathbf{k}+x\beta\mathbf{k})^2+x(1-x)\beta^2\mathbf{k}^2+m^2]^{-2}.\tag{4.41}$$

We now substitute (4.38)–(4.41) back into (4.35) and carry out the remaining $\mathbf{w}$ integrations. This can be done quite straightforwardly by first making a translation

$$\mathbf{w}''=\mathbf{w}-\tfrac{1}{2}\beta\mathbf{k}+x\beta\mathbf{k}$$

and performing the $\mathbf{w}''$ integration. The final expression is simply

$$\alpha(A^{(b)ij}+A^{(c)ij})=i(\sqrt{s})[I_{ij}(\mathbf{k},0)+C\delta_{ij}]\delta(q_-).\tag{4.42}$$

It is interesting that (4.42) is quite similar to (4.32). Since the logarithmic-divergence constant C is the same in both cases, it drops out in the final expression. This cancellation can be proved more rigorously by introducing heavy-mass regulators into the electron propagators. The final amplitude for Figs. 6(a)–6(c) is

$$\begin{aligned}\alpha A^{ij}=&-i(\sqrt{s})\\&\times[I_{ij}(-\mathbf{q}+\tfrac{1}{2}\mathbf{k},\mathbf{q}+\tfrac{1}{2}\mathbf{k})-I_{ij}(\mathbf{k},0)]\delta(q_-),\end{aligned}\tag{4.43}$$

which is perfectly finite.

Knowing the A's for both the electron (and/or positron) and for the photon, it is a simple matter to compute the asymptotic amplitudes for Compton and photon-photon scatterings [see Figs. 5(c)–5(f)] by putting A's into (4.1) and carrying out $q_\pm$ integrations. The amplitudes are

$$\begin{aligned}M(\gamma,e^{\mp})=&-\tfrac{1}{2}is\delta_{\lambda_2\lambda_4}m^{-1}e^4\int\frac{d^2q}{(2\pi)^2}\\&\times[I_{ij}(-\mathbf{q}+\tfrac{1}{2}\mathbf{k},\mathbf{q}+\tfrac{1}{2}\mathbf{k})-I_{ij}(\mathbf{k},0)]\\&\times[(\mathbf{q}+\tfrac{1}{2}\mathbf{k})^2+\mu^2]^{-1}[(\mathbf{q}-\tfrac{1}{2}\mathbf{k})^2+\mu^2]^{-1},\end{aligned}\tag{4.44}$$

$$\begin{aligned}M(\gamma\gamma)=&-ise^4\int\frac{d^2q}{(2\pi)^2}[I_{ij}(-\mathbf{q}+\tfrac{1}{2}\mathbf{k},\mathbf{q}+\tfrac{1}{2}\mathbf{k})-I_{ij}(\mathbf{k},0)]\\&\times[I_{i'j'}(\mathbf{q}-\tfrac{1}{2}\mathbf{k},-\mathbf{q}-\tfrac{1}{2}\mathbf{k})-I_{i'j'}(-\mathbf{k},0)]\\&\times[(\mathbf{q}+\tfrac{1}{2}\mathbf{k})^2+\mu^2]^{-1}[(\mathbf{q}-\tfrac{1}{2}\mathbf{k})^2+\mu^2]^{-1}.\end{aligned}\tag{4.45}$$

V. *ee* SCATTERING AMPLITUDE

Having illustrated the details of the infinite-momentum technique, we proceed to sum the multiphoton exchange diagrams shown in Fig. 1. To avoid possible confusion of signs, we remind the reader that the matrix elements or the scattering amplitudes in this paper are the *invariant T-matrix elements*. The forward elastic amplitude, in our convention, is then proportional to the energy shift of the two-particle system due to the interaction. It has a *negative* imaginary part by the optical theorem.

To evaluate the diagrams in Fig. 1, it requires only a careful counting in addition to the calculation carried out in the previous sections. For the sake of clarity, let us discuss the *ee* scattering first.

1. Matrix Elements and Their s Dependence

A special feature of the diagram in Fig. 1(a) is the following. Each photon line has one of its ends joined to the electron with large p_+, and the other end joined to that with large p_-. As a result, only γ_+ contributes at the left end and only γ_- contributes at the right end.

Let us label the photon lines starting from the bottom of the right side of Fig. 1(a) by $j=1, 2, 3, \cdots, N$. The sum of the photon momenta q_j must be the total momentum transfer k. The integrals over q_j have the

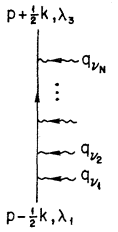

FIG. 7. Left side of Fig. 1(a).

volume element

$$(2\pi)^4 i\delta^4(\sum_{j=1}^{N} q_j - k)\prod_{j=1}^{N}\frac{d^4q_j}{(2\pi)^4 i} = 2(2\pi)^4 i\delta((\sum_{j=1}^{N} q_j)_-)$$
$$\times\delta((\sum_{j=1}^{N} q_j)_+)\delta(\sum_j \mathbf{q}_j - \mathbf{k})\prod_{j=1}^{N} dq_{j+}dq_{j-}d^2q_j$$
$$\times[2(2\pi)^4 i]^{-1}. \quad (5.1)$$

For each photon line, we have a factor

$$(q_j{}^2 - \mu^2 + i\epsilon)^{-1}. \quad (5.2)$$

The left side of the diagram in Fig. 1(a) looks like that shown in Fig. 7. The set $(\nu_1,\nu_2,\cdots,\nu_N)$ is obtained from $(1,2,\cdots,N)$ via the permutation ν. For every permutation, there is a diagram. There is a total of $N!$ diagrams with N photons exchanged.

The numerators of the electron propagators and spinors in Fig. 7 contribute the factor

$$\bar{u}_3(p+\tfrac{1}{2}k)\gamma^{\bar{\mu}_N}(\not{p}-\tfrac{1}{2}\not{k}+\not{q}_{\nu_1}+\cdots+\not{q}_{\nu_{N-1}}+m)\gamma^{\bar{\mu}_{N-1}}$$
$$\times\cdots\times\gamma^{\bar{\mu}_2}(\not{p}-\tfrac{1}{2}\not{k}+\not{q}_{\nu_1}+m)\gamma^{\bar{\mu}_1}u_1(p-\tfrac{1}{2}k), \quad (5.3)$$

with

$$\bar{\mu}_i = \mu_{\nu_i}.$$

Transforming to the standard frame with $p_+{}' = 1$, we find that the leading component is that with $\mu_1 = \mu_2 = \cdots = \mu_N = +$. Similar to (4.2), (5.3) can now be written as

$$s^{\frac{1}{2}N}\bar{u}_3(p'+\tfrac{1}{2}k)(\tfrac{1}{2}\sqrt{2}\gamma_+\tfrac{1}{2}\gamma_-)^{N-1}\tfrac{1}{2}\sqrt{2}\gamma_+u_1(p'-\tfrac{1}{2}k)$$
$$= 2^{\frac{1}{2}N-1}s^{\frac{1}{2}N}m^{-1}\delta_{\lambda_3\lambda_1} \quad (5.4)$$

for $s\to\infty$. We have made use of Eq. (2.13) and the fact that

$$(\tfrac{1}{2}\gamma_+)(\tfrac{1}{2}\gamma_-)\gamma_+ = \gamma_+, \quad (5.5)$$

and have included a $\frac{1}{2}\sqrt{2}$ for each γ_+ vertex. By similar arguments, the numerators of the electron propagators on the right side of the diagram [Fig. 1(a)] give

$$2^{\frac{1}{2}N-1}s^{\frac{1}{2}N}m^{-1}\delta_{\lambda_4\lambda_2}. \quad (5.6)$$

The jth electron propagator (from the bottom) in Fig. 7 has the denominator

$$(p-\tfrac{1}{2}k+q_{\nu_1}+q_{\nu_2}+\cdots+q_{\nu_j})^2 - m^2 + i\epsilon$$
$$= (p+q_{\nu_1}+\cdots+q_{\nu_j})_+(p+q_{\nu_2}+\cdots+q_{\nu_j})_-$$
$$-(-\tfrac{1}{2}\mathbf{k}+\mathbf{q}_{\nu_1}+\cdots+\mathbf{q}_{\nu_j})^2 - m^2 + i\epsilon. \quad (5.7)$$

Substituting $\sqrt{s}$ for p_+ and $1/\sqrt{s}$ for p_-, one finds that (5.7) reduces, at the $s\to\infty$ limit, to

$$(\sqrt{s})[(q_{\nu_1}+q_{\nu_2}+\cdots+q_{\nu_j})_- + i\epsilon] \equiv (\sqrt{s})D_{\nu_j}. \quad (5.8)$$

Thus, the $N-1$ electron propagators on the left, together with the $N-1$ electron propagators on the right, contribute a factor

$$(1/\sqrt{s})^{2N-2}, \quad (5.9)$$

which, combined with (5.4) and (5.6), gives the s to the first-power dependence of the scattering amplitude.

2. Summation over Permutations of Photon Vertices

The quantity of interest is

$$\sum_\nu (D_{\nu_1}D_{\nu_2}\cdots D_{\nu_{N-1}})\delta((\sum_j q_j)_-), \quad (5.10)$$

since there is a D_{ν_j} given by (5.8) for each electron propagator on the left and we must sum over all permutations. In (5.10), we have included a δ function appearing in (5.1) to ensure momentum conservation. Notice that the permutation ν occurs nowhere else in the amplitude except in (5.8). Therefore, the sum over the $N!$ diagrams will be accomplished when the sum over ν in (5.10) is carried out. We now show that (5.10) gives simply

$$(-2\pi i)^{N-1}\prod_{j=1}^{N}\delta(q_{j-}). \quad (5.11)$$

This result follows from the following:

Lemma.

$$\sum_\nu (w_{\nu_1}+i\epsilon)^{-1}(w_{\nu_1}+w_{\nu_2}+i\epsilon)^{-1}\times\cdots$$
$$\times(w_{\nu_1}+w_{\nu_2}+\cdots+w_{\nu_{N-1}}+i\epsilon)^{-1}\times\delta(w_1+\cdots+w_N)$$
$$= (-2\pi i)^{N-1}\prod_{j=1}^{N}\delta(w_j), \quad (5.12)$$

where w_j are real numbers. To prove (5.12), we write

$$(w+i\epsilon)^{-1} = -i\int d\tau\,\theta(\tau)e^{i(w+i\epsilon)\tau} \quad (5.13)$$

and

$$\delta(w_1+\cdots+w_N) = \frac{1}{2\pi}\int dt_N\prod_{j=1}^{N}\exp(-iw_{\nu_j}t_N). \quad (5.14)$$

Thus, the left-hand side of (5.12) is

$$(2\pi)^{-1}\sum_\nu(-i)^{N-1}\int dt_N\prod_{j=1}^{N-1}\{d\tau_j\theta(\tau_j)$$
$$\times\exp[i(\sum_{j'=1}^{j} w_{\nu_{j'}}+i\epsilon)\tau_j]\exp(-iw_{\nu_j}t_N)\}$$
$$= (2\pi)^{-1}\sum_\nu(-i)^{N-1}\int dt_1dt_2\cdots dt_N$$
$$\times\exp(-i\sum_{j=1}^{N} w_{\nu_j}t_j), \quad t_N > t_{N-1} > \cdots > t_1, \quad (5.15)$$

where we have made the change of variables from τ_i to t_i:

$$t_i = t_{i+1} - \tau_i$$

or

$$\tau_i = t_{i+1} - t_i, \quad i = 1, 2, 3, \ldots, N-1. \tag{5.16}$$

Now the sum over the permutations ν effectively eliminates the time ordering in (5.15). Integrating over t_j independently, we obtain the right-hand side of (5.12), and the lemma is proved.

This lemma can also be understood physically as follows. Consider a zero-dimensional system with zero unperturbed Hamiltonian. Under the perturbation

$$V(t) = \sum_{j=1}^{N} g_j e^{-iw_j t}, \tag{5.17}$$

where g_j are constants, the U operator is given by

$$i\frac{\partial}{\partial t} U(t,t') = V(t)U(t,t'), \tag{5.18}$$

i.e.,

$$U(t,t') = \exp\left(-i\int_{t'}^{t} dt'' \sum_j g_j e^{-iw_j t''}\right). \tag{5.19}$$

The term proportional to $g_1 g_2 \cdots g_N$ in the S matrix,

$$S = U(\infty, -\infty),$$

can be read off from (5.19). It is

$$\prod_{j=1}^{N} [-2\pi i g_j \delta(w_j)]. \tag{5.20}$$

This term in the S matrix can also be obtained via the Feynman rules by summing the diagrams geometrically identical to Fig. 6, with $(w+i\epsilon)^{-1}$ as the propagator for an internal line of energy w. In this way, one obtains $-2\pi i g_1 \cdots g_N$ times the left-hand side of (5.12). Comparing this result with (5.20), we establish (5.12) immediately.

Now let us return to the evaluation of the amplitude. By symmetry, we must have a factor

$$(-2\pi i)^{N-1} \prod_{j=1}^{N} \delta(q_{j+}) \tag{5.21}$$

for the electron denominators on the right side of the diagram in Fig. 1(a). Equation (5.21) can be obtained by permuting the vertices on the right side in all possible ways. However, when one permutes the vertices on both sides in all possible ways, each diagram appears $N!$ times corresponding to $N!$ sets of labeling. Thus, a factor $(N!)^{-1}$ must be included. Combining (5.1), (5.2), (5.4), (5.6), (5.11), and (5.21) and integrating over the q's, we obtain the N-photon exchange ee amplitude

$$\begin{aligned} &-s(N!)^{-1}\delta_{\lambda_3\lambda_1}\delta_{\lambda_4\lambda_2} m^{-2} 2^{N-2} (2\pi i)^{2N-2} 2(2\pi)^4 i \\ &\times \int \prod_{j=1}^{N} d^2q_j dq_{j+} dq_{j-} [2(2\pi)^4 i]^{-1} \delta(q_{j+})\delta(q_{j-}) \\ &\times (-\mathbf{q}_j^2 - \mu^2 + i\epsilon)^{-1} \delta\Big(\sum_i \mathbf{q}_i - \mathbf{k}\Big) \\ &= \tfrac{1}{2} i s \delta_{\lambda_3\lambda_1}\delta_{\lambda_4\lambda_2} m^{-2} \int d^2b\, e^{-i\mathbf{k}\cdot\mathbf{b}} (N!)^{-1} [i\chi(\mathbf{b})]^N, \end{aligned} \tag{5.22}$$

where we have defined

$$\chi(\mathbf{b}) = -e^2 \int \frac{d^2q}{(2\pi)^2} (\mathbf{q}^2+\mu^2)^{-1} e^{i\mathbf{q}\cdot\mathbf{b}}. \tag{5.23}$$

It can be shown easily that, for e^+e^- scattering, one simply changes χ to $-\chi$. Summing over N from 1 to infinity, we have, for the ee scattering amplitude,

$$M(e^-e^{\mp}) = \tfrac{1}{2} i s \delta_{\lambda_3\lambda_1}\delta_{\lambda_4\lambda_2} m^{-2} F_{\pm}'(\mathbf{k}), \tag{5.24}$$

where $F_{\pm}'$ is defined by the eikonal form

$$\begin{aligned} F_{\pm}'(\mathbf{k}) &= \int d^2b\, e^{-i\mathbf{b}\cdot\mathbf{k}} (e^{\pm i\chi(\mathbf{b})} - 1) \\ &\equiv F_{\pm}(\mathbf{k}) - (2\pi)^2 \delta(\mathbf{k}). \end{aligned} \tag{5.25}$$

3. Semiclassical Feature

The amplitude $M(e^-e^{\mp})$ has the simple eikonal form expected from the semiclassical approximation. In Ref. 1, it is shown that, in the semiclassical approximation, $\chi(\mathbf{b})$ is given by

$$\chi(\mathbf{b}) = -v^{-1} \int_{-\infty}^{\infty} dz\, V(\mathbf{b}+\mathbf{z}) \tag{5.26}$$

for the scattering of a particle by the potential $V(\mathbf{r})$. In (5.26), v is the velocity of the particle, which moves in the z direction, and $\mathbf{b}$ is the impact parameter specifying the position of the particle trajectory with respect to the center of the potential. If we set the potential to be

$$\begin{aligned} V(\mathbf{r}) &= e^2 (4\pi r)^{-1} e^{-\mu r} \\ &= e^2 \int d^3q (2\pi)^{-3} (\mathbf{q}^2+\mu^2)^{-1} e^{i\mathbf{q}\cdot\mathbf{r}}, \end{aligned} \tag{5.27}$$

which is a Coulomb potential in the limit $\mu \to 0$, then (5.26) leads to (5.23). The velocity v in (5.26) does not have a definite relativistic generalization. To get (5.23), we must set it equal to 1. Notice that there is no argument against writing v as p/m, which has a completely different asymptotic form $(\sqrt{s})/m$. One does not expect to obtain a definite relativistic answer from (5.26), which basically is a nonrelativistic result.

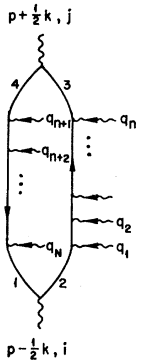

FIG. 8. Left side of Fig. 1(b).

The fact that (5.24) turns out to have the eikonal form of the semiclassical approximation is not surprising. This is because, in going from (5.7) to (5.8), we have dropped, among other things, the q_j^2 terms in the propagators. The dropping of q_j^2 terms is a crucial step in the semiclassical approximation, and corresponds to neglecting the effect of recoil. For the details of the semiclassical approximation, see, for example, Ref. 1.

At this point we would like to emphasize that the appearance of the eikonal form in the *ee* scattering amplitude is a consequence of the fact that the exchanged particles, i.e., the photons, are of spin 1. If, instead of photons, scalar particles are exchanged, it can be shown that no meaningful eikonal form can be obtained from summing the same set of diagrams. If one goes through the above calculations with the photon replaced by a scalar particle, one would find $\chi(\mathbf{b})=O(s^{-1})$ instead of $O(1)$, which is of the same order as the neglected terms.

4. Ladder Diagrams

The ladder diagrams play an important role in many model calculations. We shall give here a qualitative discussion of the *ee* scattering ladder diagrams, which form a subset of the multiphoton exchange diagrams we just summed. What we want to demonstrate is that the sum over a different set of diagrams can give entirely different s dependence of the amplitude. The result of the ladder sum has no meaning here since, as will be seen in Sec. VII, the set of ladder diagrams does not satisfy gauge invariance.

The calculation of ladder diagrams turns out to be more complicated than the above calculation. In the above calculation, δ functions in $q_{j\pm}$ were obtained after summing the permutations of photon vertices. For ladder diagrams, no such permutation exists and one obtains powers of $\ln s$ instead of δ functions. To illustrate this, consider the two-photon ladder shown in Fig. 5(a).

The algebra proceeds in the same way as that described in Sec. IV. The denominators of the two-electron propagators give

$$\{-[(\sqrt{s})-q_+]q_--\mathbf{q}^2-m^2+i\epsilon\}^{-1}\times\{[(\sqrt{s})+q_-]q_+-\mathbf{q}^2-m^2+i\epsilon\}^{-1}. \quad (5.28)$$

Here we are keeping the $O(q^2/\sqrt{s})$ terms in (4.7). If these terms are ignored, we would get

$$\int_0^\infty \frac{dq_+}{q_+} \quad (5.29)$$

after performing the q_- integral. Equation (5.29) is logarithmically divergent. Keeping all terms in (5.28), the $q_\pm$ integrals then give

$$\int_0^{\sqrt{s}} dq_+[(\sqrt{s})q_+-(\mathbf{q}^2+m^2-i\epsilon)]^{-1}=(1/\sqrt{s})[\ln s+O(1)]. \quad (5.30)$$

The resultant amplitude is already given by (4.12). When more photons are exchanged, the calculation gets involved. Rough estimates show that, for the N-photon exchange ladder, the leading term is

$$-\delta_{\lambda_3\lambda_1}\delta_{\lambda_4\lambda_2}m^{-2}s(\tfrac{1}{2}\pi^{-1}\ln s)^{N-1}\int d^2b\, e^{-i\mathbf{k}\cdot\mathbf{b}}\chi(\mathbf{b})^N. \quad (5.31)$$

Summing over N formally, one obtains an $s/\ln s$ behavior, which might look like what is expected from a Regge cut. The spurious $\ln s$ terms are manifestly absent when diagrams with crossed photon lines are included. As was already mentioned, it will be shown later that the ladder diagrams do not satisfy gauge invariance and should not be taken seriously.

VI. $e\gamma$ AND $\gamma\gamma$ SCATTERING AMPLITUDES

The procedure shown in the previous section can also be carried out to sum the diagrams shown in Figs. 1(b) and 1(c). Consider the electron-photon scattering first.

Figure 8 shows the left side of Fig. 1(b) in detail. There are N internal photon lines labeled by $q_1, \ldots, q_N$. The photon lines $1, \ldots, n$ end on the upward line of the loop and the rest of the photon lines, $n+1, \ldots, N$, end on the downward line. The free ends of these N photons are to be joined to the electron line on the right in all possible orders to form Fig. 1(b).

As before, we need to consider the term with γ_+ at each of these N vertices in Fig. 8. There are $n-1$ electron propagators between n and 1. Only the term proportional to γ_- in the numerator of each of these propagators can survive between the γ_+'s sandwiching the propagators. From these $n-1$ numerators and the n vertices, we get the factor

$$(w_+'s^{\frac{1}{2}})^{n-1}(\tfrac{1}{2}\sqrt{2}\gamma_+\tfrac{1}{2}\gamma_-)^{n-1}\tfrac{1}{2}\sqrt{2}\gamma_+ = 2^{\frac{1}{2}n-1}(w_+'s^{\frac{1}{2}})^{n-1}\gamma_+, \quad (6.1)$$

after transforming to the standard frame. Similarly,

for the $N-n$ vertices and the numerators of the $N-n-1$ electron propagators sandwiched by them on the downward line, we have the factor

$$2^{\frac{1}{2}(N-n)-1}[(w_+'-1)s^{\frac{1}{2}}]^{N-n-1}\gamma_+. \tag{6.2}$$

Therefore, apart from numerical constants, these two groups of vertices and propagators behave like two γ_+ vertices with momentum inputs

$$\begin{aligned} &q_1+q_2+\cdots+q_n\equiv k_1 \\ \text{and} \qquad &\\ &q_{n+1}+\cdots+q_N\equiv k_2, \end{aligned} \tag{6.3}$$

respectively, on the two sides of the loop. Of course, we have

$$k_1+k_2=k. \tag{6.4}$$

The remaining four electron propagators, which are joined to the external photon lines, can be analyzed in exactly the same way as was done in Sec. IV. The relevant quantity is the same as (4.14), with the substitution

$$-q+\tfrac{1}{2}k\to k_1, \quad q+\tfrac{1}{2}k\to k_2, \tag{6.5}$$

and with the two γ_+'s supplied by (6.1) and (6.2). All the algebra following (4.14) goes through. In particular, the $\delta(q_-)$ in (4.25) implies, by (6.5) and (6.3), that the factor

$$\begin{aligned} \delta(k_{1-}) &= \delta(k_{2-}) \\ &= \delta\Big(\Big(\sum_{j=1}^{n} q_j\Big)_-\Big) \\ &= \delta\Big(\Big(\sum_{j=n+1}^{N} q_j\Big)_-\Big) \end{aligned} \tag{6.6}$$

appears. In (6.6), we have utilized (6.3) and (6.4). Also, the variable w_+' is restricted between 0 and 1 as before.

The denominator of the electron propagator between the vertices j and $j+1$ with $1\le j\le n-1$ is

$$\begin{aligned} (w-\tfrac{1}{2}k+q_1+q_2+q_j)^2-m^2+i\epsilon &\\ =(\sqrt{s})w_+'[(q_1+\cdots+q_j)_-+i\epsilon] &\\ \equiv(\sqrt{s})w_+'D_j & \end{aligned} \tag{6.7}$$

as $s\to\infty$. Similarly, the denominator of the electron propagator with $n+1\le j\le N-1$ is

$$\begin{aligned} (w-p-k+k_1+q_{n+1}+\cdots+q_j)^2-m^2+i\epsilon &\\ =(\sqrt{s})(w_+'-1)[(q_{n+1}+\cdots+q_j)_--i\epsilon] &\\ \equiv(\sqrt{s})(w_+'-1)D_j'. & \end{aligned} \tag{6.8}$$

We have made use of the fact that $k_{1-}=k_{2-}=k_-=0$ and that $0<w_+'<1$.

The $(\sqrt{s})w_+'$ and $(\sqrt{s})(w_+'-1)$ factors in the denominators given by (6.7) and (6.8) cancel the corresponding factors in the numerators summarized by (6.1) and (6.2). What remains after combining (6.1) and (6.2) with (6.7) and (6.8) is

$$2^{\frac{1}{2}n-1}(D_1D_2\cdots D_{n-1})^{-1}2^{\frac{1}{2}(N-n)-1}(D_{n+1}'\cdots D_{N-1}')^{-1}, \tag{6.9}$$

which multiplies the quantity (4.14) with the substitution (6.5) mentioned above.

The next step is to sum the diagrams with different orderings of the vertices. This can be done in the same fashion as the *ee* diagrams were summed in the previous section.

First, we permute the indices $j=1, 2, \ldots, n$ in all possible ways, i.e., we replace D_j in (6.9) by D_{ν_j} [defined by (5.8)] and sum over all the permutations. Because of the presence of $\delta((q_1+\cdots+q_n)_-)$ [see (6.6)] and the identity (5.12), we have

$$\begin{aligned} &2^{\frac{1}{2}n-1}\sum_{\nu}(D_{\nu_1}D_{\nu_2}\cdots D_{\nu_{n-1}})^{-1} \\ &\qquad=2^{\frac{1}{2}n-1}(-2\pi i)^{n-1}\prod_{j=1}^{n-1}\delta(q_{j-}). \end{aligned} \tag{6.10}$$

Next, we permute the indices $j=n+1, n+2, \ldots, N$ in all possible ways and sum over the permutations. Due to the presence of $\delta((q_{n+1}+\cdots+q_N)_-)$ [again, see (6.6)] and (5.12), we have for the second factor in (6.9)

$$2^{\frac{1}{2}(N-n)-1}(2\pi i)^{N-n-1}\prod_{j=n+1}^{N-1}\delta(q_{j-}). \tag{6.11}$$

The appearance of $2\pi i$ in (6.11) instead of $-2\pi i$ is because the D_j' in (6.8) has a negative imaginary part $-i\epsilon$ instead of a positive $+i\epsilon$. Finally, we permute the N vertices on the electron line on the right side of the diagram and sum over the permutations. We obtain, as we did in the previous section,

$$2^{\frac{1}{2}N-1}(-2\pi i)^{N-1}\prod_{j=1}^{N}\delta(q_{j+}). \tag{6.12}$$

The above permutations in fact count every diagram $n!(N-n)!$ times. One way to see this is the following. The $N!$ permutations of the vertices on the right include those permuting within each of the two subsets of vertices of photon lines joining, respectively, the upward and the downward lines of the loop. Thus, when the vertices on either side of the loop are then permuted among themselves, one obtains no new diagrams but interchanges of labels. Therefore, every diagram appears $n!(N-n)!$ times during the permutation.

Let us summarize the above results and obtain the final form of the γe scattering amplitude:

(1) For the fermion loop, we have

$$\begin{aligned} e^2i(2\pi)^{-4}\int d^4w\, M_{ij}(k_1,k_2;w) &= -i(\sqrt{s})4\pi \\ &\times[I_{ij}(\mathbf{k}_1,\mathbf{k}_2)+C\delta_{ij}]\delta((q_1+\cdots+q_n)_-). \end{aligned} \tag{6.13}$$

See (4.32) and the discussion between (6.1) and (6.5).

(2) For the electron line on the right, there is the factor

$$(\sqrt{s})\delta_{\lambda_4\lambda_2}m^{-1}. \tag{6.14}$$

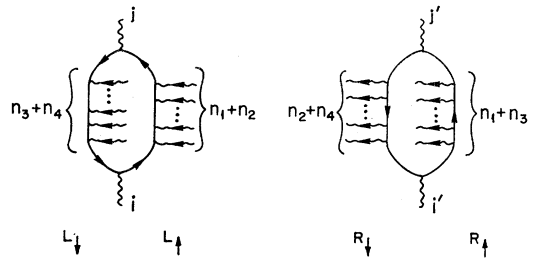

FIG. 9. Loops in Fig. 1(c) shown in more detail.

(3) For the N internal photon lines, since $q_{j\pm}=0$, we have a factor

$$\prod_{j=1}^{N}(-\mathbf{q}_j{}^2-\mu^2)^{-1}. \tag{6.15}$$

(4) The q_j integrals take the form

$$(2\pi)^4 i\delta^4(\sum_i q_i-k)\prod_{j=1}^{N}\frac{d^4q_j}{(2\pi)^4 i}.$$

The $q_\pm$ integrals in the above form can be evaluated trivially with the help of the δ functions in (6.6) and (6.10)–(6.12), giving a factor

$$\tfrac{1}{4}(2\pi)^{-1}(-)^n(2\pi)^2\delta(\sum_{i=1}^{N}\mathbf{q}_i-\mathbf{k})\prod_{j=1}^{N}\frac{d^2q_j}{(2\pi)^2 i}. \tag{6.16}$$

The $\mathbf{q}_j$ integrals can also be written as

$$\int d^2k_1 d^2k_2(2\pi)^{-2}\delta(\mathbf{k}-\mathbf{k}_1-\mathbf{k}_2)(2\pi)^2\delta(\mathbf{k}_1-\sum_{i=1}^{n}\mathbf{q}_i)$$

$$\times\prod_{j=1}^{n}\frac{d^2q_j}{(2\pi)^2 i}(2\pi)^2\delta(\mathbf{k}_2-\sum_{l=n+1}^{N}\mathbf{q}_l)\prod_{m=n+1}^{N}\frac{d^2q_m}{(2\pi)^2 i}. \tag{6.17}$$

(5) There is an over-all counting factor of

$$[n!(N-m)!]^{-1}. \tag{6.18}$$

Combining (6.13)–(6.18), we obtain the γe scattering amplitude with N photons exchanged

$$-\sum_{n=0}^{N}\tfrac{1}{2}is\delta_{\lambda_4\lambda_2}m^{-1}\int d^2k_1 d^2k_2\,(2\pi)^{-2}\delta(\mathbf{k}-\mathbf{k}_1-\mathbf{k}_2)$$

$$\times\int d^2b_1 e^{-i\mathbf{b}_1\cdot\mathbf{k}_1}[i\chi(\mathbf{b}_1)]^n\int d^2b_2 e^{-i\mathbf{b}_2\cdot\mathbf{k}_2}[-i\chi(\mathbf{b}_2)]^{N-n}$$

$$\times[n!(N-n)!]^{-1}[I_{ij}(\mathbf{k}_1,\mathbf{k}_2)+C\delta_{ij}], \tag{6.19}$$

where χ is given by (5.23).

Notice that our discussion in this section has been restricted to the case $n\neq 0$ and $n\neq N$. However, one can easily check that (6.19) is valid for $n=0$, N too. The constant C in (6.19) does not contribute since the term involving C is proportional to

$$C\delta(\mathbf{b}_1-\mathbf{b}_2)\sum_{n=0}^{N}[n!(N-n)!]^{-1}\chi(\mathbf{b}_1)^n[-\chi(\mathbf{b}_2)]^{N-n}$$

$$=C\delta(\mathbf{b}_1-\mathbf{b}_2)[\chi(\mathbf{b}_1)-\chi(\mathbf{b}_2)]^N(N!)^{-1}$$

$$=0. \tag{6.20}$$

The factor $\delta(\mathbf{b}_1-\mathbf{b}_2)$ comes from the $\mathbf{k}_1$, $\mathbf{k}_2$ integrals.

Summing over n and N in (6.19), we obtain the final form of the γe scattering amplitude:

$$M(\gamma e)=-\tfrac{1}{2}is\delta_{\lambda_4\lambda_2}m^{-1}\int d^2k_1 d^2k_2(2\pi)^{-4}\delta(\mathbf{k}_1+\mathbf{k}_2-\mathbf{k})$$

$$\times[F_+(\mathbf{k}_1)F_-(\mathbf{k}_2)-(2\pi)^4\delta(\mathbf{k}_1)\delta(\mathbf{k}_2)]I_{ij}(\mathbf{k}_1,\mathbf{k}_2), \tag{6.21}$$

where $F_\pm$ are given by (5.25).

The summation of the diagrams like Fig. 1(c) for the $\gamma\gamma$ scattering amplitude is a straightforward extension of the above analysis. Let us consider the case where N photons are exchanged.

In Fig. 1(c), each of the two loops has two sides with electron lines pointing up and down, respectively. Let us label these four sides by $L_\uparrow$, $L_\downarrow$, $R_\uparrow$, and $R_\downarrow$, respectively (see Fig. 9).

Let us group the N exchanged photons into four sets, 1, 2, 3, and 4, including n_1, n_2, n_3, and n_4 photons carrying the momenta k_1, k_2, k_3, and k_4 from the sides $R_\uparrow$, $R_\downarrow$, $R_\uparrow$, and $R_\downarrow$ to the sides $L_\uparrow$, $L_\uparrow$, $L_\downarrow$, and $L_\downarrow$, respectively. Of course,

$$\sum_{l=1}^{4}n_l=N,\qquad \sum_{l=1}^{4}k_l=k. \tag{6.22}$$

The number of vertices on the four sides are, excluding the four external photon vertices (see Fig. 9).

$$n_1+n_2 \text{ on } L_\uparrow,\quad n_3+n_4 \text{ on } L_\downarrow,\qquad n_1+n_3 \text{ on } R_\uparrow,\quad n_2+n_4 \text{ on } R_\downarrow. \tag{6.23}$$

Going through the same argument leading to (6.1)–(6.3), one sees that these four sets of vertices behave like four vertices one on each side, i.e., a γ_+ on $L_\uparrow$, a γ_+ on $L_\downarrow$, a γ_- on $R_\uparrow$, and a γ_- on $R_\downarrow$. The analysis through (6.11) for the loop in Fig. 8 clearly applies, with obvious modifications in notation, to the left loop here. The results for the right loop can be easily obtained via symmetry arguments from those for the left loop.

Permuting the vertices on each of the four sides in all possible ways, we get the product of $\delta(q_{j-})$'s and $\delta(q_{j+})$'s similar to (6.10) and (6.11). The coefficient in front of the δ functions is a product of four factors corresponding

to the four sides, that is,

$$2^{\frac{1}{2}(n_1+n_2)-1}(-2\pi i)^{n_1+n_2-1}2^{\frac{1}{2}(n_3+n_4)-1}(2\pi i)^{n_3+n_4-1}$$
$$\times 2^{\frac{1}{2}(n_1+n_3)-1}(-2\pi i)^{n_1+n_3-1}2^{\frac{1}{2}(n_2+n_4)-1}(2\pi i)^{n_2+n_4-1}$$
$$=2^{N-4}(2\pi)^{2N-4}(-)^{n_1+n_4}. \quad (6.24)$$

We have actually counted each diagram $n_1!n_2!n_3!n_4!$ times in the above permutations. One way to see this is the following. When one permutes the vertices on each of the four sides independently, the permutations within set 1, for example, include those which correspond to the relabeling of diagrams. There are $n_1!$ such relabelings in set 1. Therefore, every diagram is counted $n_1!n_2!n_3!n_4!$ times.

For the photon propagators, we again have (6.15). For the two loop integrals, we have

$$i(2\pi)^{-4}\int dw\, M_{ij}(k_1+k_2, k_3+k_4; w) \quad (6.25)$$

and

$$i(2\pi)^{-4}\int dw\, M_{i'j'}(k_1+k_3, k_2+k_4; w), \quad (6.26)$$

respectively.

Combining (6.24)–(6.26), we find that the contribution to the $\gamma\gamma$ scattering amplitude by the diagrams with given n_1, n_2, n_3, and n_4 is

$$\tfrac{1}{2}is\int(2\pi)^2\delta(\mathbf{k}-\sum_{l=1}^{4}\mathbf{k}_l)\Big\{\prod_{l=1}^{4}d^2k_l(2\pi)^{-2}d^2b_l e^{-i\mathbf{b}_l\cdot\mathbf{k}_l}$$
$$\times\frac{1}{n_l!}[i\chi(\mathbf{b}_l)]^{n_l}\Big\}(-)^{n_2+n_3}I_{ij}(\mathbf{k}_1+\mathbf{k}_2, \mathbf{k}_3+\mathbf{k}_4)$$
$$\times I_{i'j'}(\mathbf{k}_1+\mathbf{k}_3, \mathbf{k}_2+\mathbf{k}_4). \quad (6.27)$$

We have used (4.32) to express (6.25) and (6.26) in terms of the I's. By the same argument leading to (6.20), it can be shown easily that the constant C does not contribute.

Summing over the n_l's in (6.27), we obtain the final form for the $\gamma\gamma$ scattering amplitude:

$$M(\gamma\gamma)=\tfrac{1}{2}is(2\pi)^{-6}\int d^2k_1d^2k_2d^2k_3d^2k_4$$
$$\times\delta(\mathbf{k}-\mathbf{k}_1-\mathbf{k}_2-\mathbf{k}_3-\mathbf{k}_4)[F_+(\mathbf{k}_1)F_-(\mathbf{k}_2)F_-(\mathbf{k}_3)F_+(\mathbf{k}_4)$$
$$-(2\pi)^8\delta(\mathbf{k}_1)\delta(\mathbf{k}_2)\delta(\mathbf{k}_3)\delta(\mathbf{k}_4)]I_{ij}(\mathbf{k}_1+\mathbf{k}_2, \mathbf{k}_3+\mathbf{k}_4)$$
$$\times I_{i'j'}(\mathbf{k}_1+\mathbf{k}_3, \mathbf{k}_2+\mathbf{k}_4). \quad (6.28)$$

The summation of the multiphoton exchange diagrams is thus completed.

Note added in proof. It is instructive to examine the $M(\gamma e)$ and $M(\gamma\gamma)$ in the impact parameter representation. Let us introduce the scattering amplitude in the impact parameter space as

$$M(\mathbf{b})=\int\frac{d^2k}{(2\pi)^2}e^{i\mathbf{k}\cdot\mathbf{b}}M(\mathbf{k}), \quad (6.29)$$

and the photon impact factor as

$$I_{ij}(\mathbf{b}_1,\mathbf{b}_2)=\int\frac{d^2k_1}{(2\pi)^2}\frac{d^2k_2}{(2\pi)^2}e^{i(\mathbf{k}_1\cdot\mathbf{b}_1+\mathbf{k}_2\cdot\mathbf{b}_2)}I_{ij}(\mathbf{k}_1,\mathbf{k}_2). \quad (6.30)$$

It is straightforward to verify that, in the impact parameter space,

$$M_{e^-e^\mp}(\mathbf{b})=\tfrac{1}{2}is\delta_{\lambda_4\lambda_2}\delta_{\lambda_3\lambda_1}m^{-2}(e^{\pm i\chi(\mathbf{b})}-1),$$

$$M_{\gamma e}(\mathbf{b})=-\tfrac{1}{2}is\delta_{\lambda_4\lambda_2}m^{-1}\int d^2b_1d^2b_2\, I_{ij}(\mathbf{b}_1,\mathbf{b}_2)$$
$$\times[e^{i\chi(\mathbf{b}-\mathbf{b}_1)-i\chi(\mathbf{b}-\mathbf{b}_2)}-1], \quad (6.31)$$

$$M_{\gamma\gamma}(\mathbf{b})=\tfrac{1}{2}is\int d^2b_1d^2b_2d^2b_3d^2b_4\, I(\mathbf{b}_1,\mathbf{b}_2)I(\mathbf{b}_3,\mathbf{b}_4)$$
$$\times[e^{i\chi(\mathbf{b}+\mathbf{b}_1-\mathbf{b}_3)-i\chi(\mathbf{b}+\mathbf{b}_1-\mathbf{b}_4)-i\chi(\mathbf{b}+\mathbf{b}_2-\mathbf{b}_3)+i\chi(\mathbf{b}+\mathbf{b}_2-\mathbf{b}_4)}-1].$$

The physical interpretation of these formulas is very clear. The impact factor $I(\mathbf{b}_1,\mathbf{b}_2)$ describes the positions of a virtual electron-position pair in the photon at the time of scattering. The total phase shift of the scattering amplitude of an electron (or a photon) with a photon is the sum of its individual phase shifts of the electron with the virtual pair, added coherently. It is interesting to see that when one substitutes Eq. (4.33) in Eq. (6.30), the integrand of $I(\mathbf{b}_1,\mathbf{b}_2)$ vanishes identically except at $\beta'\mathbf{b}_1+\beta\mathbf{b}_2=0$. For relativistic moving electron and positron, β' and β are proportional to their relativistic energy. The above relation is simply a restriction imposed by the constancy of the center of mass of the virtual pair.

VII. EXPLICIT EXPRESSIONS AND GAUGE INVARIANCE

1. Functions $F_\pm$ and ee Amplitude

The factors $F_\pm$ occur in all of our formulas for the scattering amplitudes. The explicit evaluation of the integrals

$$F_\pm'(k)=\int d^2b\, e^{-i\mathbf{k}\cdot\mathbf{b}}(e^{\pm i\chi(\mathbf{b})}-1), \quad (7.1)$$

$$\chi(\mathbf{b})=-e^2\int d^2q(2\pi)^{-2}(\mathbf{q}^2+\mu^2)^{-1}e^{i\mathbf{q}\cdot\mathbf{b}}$$
$$=-2\alpha K_0(\mu b) \quad (7.2)$$

is straightforward. The result, in the limit $\mu^2 \to 0$, is

$$\chi(\mathbf{b}) = \alpha[2\ln(\tfrac{1}{2}b\mu) + 2\gamma + \tfrac{1}{2}\mu^2 b^2 \ln(\tfrac{1}{2}b\mu) + O(b^2\mu^2)], \quad (7.3)$$

$$F_\pm'(k) = \mp i(e^2/\mathbf{k}^2)e^{\mp i\Delta(\mathbf{k})}, \quad (7.4)$$

$$\Delta(\mathbf{k}) = \alpha[\ln(\mathbf{k}^2/\mu^2) - 2\gamma] - 2\eta, \quad (7.5)$$

where $\alpha = e^2/4\pi$, $\gamma \approx 0.577$ is Euler's constant, and

$$\eta = \arg\Gamma(1+i\alpha). \quad (7.6)$$

Since μ plays the role of a photon mass, it must be let go to zero in the final expressions of scattering amplitudes.

For the *ee* scattering amplitudes, we have, by (5.24) and (7.4),

$$M(e^-e^\mp) = \tfrac{1}{2}is\delta_{\lambda_3\lambda_1}\delta_{\lambda_4\lambda_2}m^{-2}F_\pm'(\mathbf{k}) = \pm\tfrac{1}{2}s\delta_{\lambda_3\lambda_1}\delta_{\lambda_4\lambda_2}m^{-2}(e^2/\mathbf{k}^2)e^{\mp\Delta(\mathbf{k})} \quad (7.7)$$

for $k \neq 0$. Equation (7.7) is simply the one-photon exchange amplitude multiplied by a phase factor. When the cross section is computed, the phase factor drops out. Thus, summing the multiphoton exchange diagrams introduces no new physical effect to the lowest-order term. This result is not unexpected, since a similar situation occurs in nonrelativistic Coulomb scattering.

The phase $\Delta(\mathbf{k})$ does have physical consequences in the γe and $\gamma\gamma$ scatterings, as is indicated in the following discussion.

2. γe, Delbrück, and $\gamma\gamma$ Scatterings

For reference, let us list (6.21) and (6.28) here.

$$M(\gamma e) = -\tfrac{1}{2}is\delta_{\lambda_4\lambda_2}m^{-1}\int d^2k_1 d^2k_2 (2\pi)^{-2}\delta(\mathbf{k}_1+\mathbf{k}_2-\mathbf{k}) \times[F_+(\mathbf{k}_1)F_-(\mathbf{k}_2) - (2\pi)^4\delta(\mathbf{k}_1)\delta(\mathbf{k}_2)] \times I_{ij}(\mathbf{k}_1,\mathbf{k}_2), \quad (7.8)$$

$$M(\gamma\gamma) = \tfrac{1}{2}is(2\pi)^{-6}\int d^2k_1 d^2k_2 d^2k_3 d^2k_4 \times\delta(\mathbf{k}_1+\mathbf{k}_2+\mathbf{k}_3+\mathbf{k}_4-\mathbf{k})[F_+(\mathbf{k}_1)F_-(\mathbf{k}_2)F_-(\mathbf{k}_3)F_+(\mathbf{k}_4) - (2\pi)^8\delta(\mathbf{k}_1)\delta(\mathbf{k}_2)\delta(\mathbf{k}_3)\delta(\mathbf{k}_4)]I_{ij}(\mathbf{k}_1+\mathbf{k}_2, \mathbf{k}_3+\mathbf{k}_4) \times I_{i'j'}(\mathbf{k}_1+\mathbf{k}_3, \mathbf{k}_2+\mathbf{k}_4). \quad (7.9)$$

It is clear from (4.33), the definition of $I_{ij}(\mathbf{k}_1,\mathbf{k}_2)$, that

$$I_{ij}(\mathbf{k}_1,\mathbf{k}_2) = I_{ji}(\mathbf{k}_1,\mathbf{k}_2) = I_{ij}(\mathbf{k}_2,\mathbf{k}_1). \quad (7.10)$$

Let us define the convolution product of the functions $A_i(\mathbf{k})$ as

$$A_1 * A_2 * \cdots * A_n = \int \delta\Big(\sum_{j=1}^n \mathbf{k}_j - \mathbf{k}\Big)\prod_{i=1}^n \frac{d^2k_i}{(2\pi)^2}A_i(\mathbf{k}_i). \quad (7.11)$$

From (7.1), one easily verifies that

$$F_+ * F_- = (2\pi)^2\delta(\mathbf{k}), \qquad F_+' * F_-' + F_+' + F_-' = 0. \quad (7.12)$$

It follows from (7.12) that (7.8) vanishes if I_{ij} is replaced by a constant or any expression independent of the individual integration variables $\mathbf{k}_1$ and $\mathbf{k}_2$. It also follows that (7.9) vanishes if one or both of the two I functions are replaced by a constant or anything independent of the four integration variables $\mathbf{k}_i$, $i = 1, \ldots, 4$. Consequently, (7.8) and (7.9) remain unchanged if we replace I_{ij} by

$$I_{ij}'(\mathbf{k}_1,\mathbf{k}_2) \equiv I_{ij}(\mathbf{k}_1,\mathbf{k}_2) - I_{ij}(\mathbf{k}_1+\mathbf{k}_2, 0), \quad (7.13)$$

because the second term on the right-hand side of (7.13) will depend only on $\mathbf{k}$, owing to the δ functions in (7.8) and (7.9), and not on the integration variables $\mathbf{k}_i$. The form factor I' is proportional to the function $\mathcal{J}_\gamma$ introduced in Ref. 4.

Using (7.12) and (7.13), it is easy to show that (7.8) can be written in terms of $F_\pm'$ as

$$M(\gamma e) = -\tfrac{1}{2}is\delta_{\lambda_4\lambda_2}m^{-1}\int d^2k_1 d^2k_2 (2\pi)^{-2}\delta(\mathbf{k}_1+\mathbf{k}_2-\mathbf{k}) \times F_+'(\mathbf{k}_1)F_-'(\mathbf{k}_2)I_{ij}'(\mathbf{k}_1,\mathbf{k}_2) = -\tfrac{1}{2}is\delta_{\lambda_4\lambda_2}m^{-1}\int d^2k_1 d^2k_2 (2\pi)^{-2}\delta(\mathbf{k}_1+\mathbf{k}_2-\mathbf{k}) \times e^4(\mathbf{k}_1^2)^{-1-i\alpha}(\mathbf{k}_2^2)^{-1+i\alpha}I_{ij}'(\mathbf{k}_1,\mathbf{k}_2). \quad (7.14)$$

Since I_{ij}' vanishes when one of $\mathbf{k}_1$, $\mathbf{k}_2$ vanishes, the integral in (7.14) is well defined. We have used the explicit expression (7.4) in obtaining the last expression in (7.14). Equation (7.14) can be easily generalized to obtain the Delbrück scattering amplitude. One simply replaces the α in (7.14) by $Z\alpha$, where Z is the nuclear charge. The result agrees with that given in Ref. 4.

The $\gamma\gamma$ scattering amplitude (7.9) can also be expressed in terms of I' and $F_\pm'$. A little algebra shows that

$$M(\gamma\gamma) = -is\int d^2k_1 d^2k_2 (2\pi)^{-2}\delta(\mathbf{k}-\mathbf{k}_1-\mathbf{k}_2) \times F_+'(\mathbf{k}_1)F_-'(\mathbf{k}_2)I_{ij}'(\mathbf{k}_1,\mathbf{k}_2)I_{i'j'}'(\mathbf{k}_1,\mathbf{k}_2) + \tfrac{1}{2}is\int d^2k_1 d^2k_2 d^2k_3 d^2k_4 (2\pi)^{-6}\delta(\mathbf{k}-\mathbf{k}_1-\mathbf{k}_2-\mathbf{k}_3-\mathbf{k}_4) \times F_+'(\mathbf{k}_1)F_-'(\mathbf{k}_2)F_-'(\mathbf{k}_3)F_+'(\mathbf{k}_4) \times J_{iji'j'}(\mathbf{k}_1,\mathbf{k}_2,\mathbf{k}_3,\mathbf{k}_4), \quad (7.15)$$

where

$$J_{iji'j'}(\mathbf{k}_1,\mathbf{k}_2,\mathbf{k}_3,\mathbf{k}_4)$$
$$=\tfrac{1}{2}[I_{ij}'(\mathbf{k}_1+\mathbf{k}_2,\,\mathbf{k}_3+\mathbf{k}_4)+I_{ij}'(\mathbf{k}_1+\mathbf{k}_3,\,\mathbf{k}_2+\mathbf{k}_4)$$
$$-I_{ij}'(\mathbf{k}_2+\mathbf{k}_3+\mathbf{k}_4,\,\mathbf{k}_1)-I_{ij}'(\mathbf{k}_1+\mathbf{k}_2+\mathbf{k}_3,\,\mathbf{k}_4)]$$
$$\times[I_{i'j'}'(\mathbf{k}_1+\mathbf{k}_3,\,\mathbf{k}_2+\mathbf{k}_4)+I_{i'j'}'(\mathbf{k}_1+\mathbf{k}_2,\,\mathbf{k}_3+\mathbf{k}_4)$$
$$-I_{i'j'}'(\mathbf{k}_1+\mathbf{k}_3+\mathbf{k}_4,\,\mathbf{k}_2)-I_{i'j'}'(\mathbf{k}_1+\mathbf{k}_2+\mathbf{k}_4,\,\mathbf{k}_3)].$$

It is clear that $J_{iji'j'}$ vanishes whenever one or more of $\mathbf{k}_1$, $\mathbf{k}_2$, $\mathbf{k}_3$, $\mathbf{k}_4$ vanishes. Therefore, (7.15) is well defined even though $F_\pm'(\mathbf{k}_1)$ blows up at $k_i=0$. In other words, there is no infrared-divergence problem here.

3. Gauge Invariance

What we have done so far is the summation of a selected set of diagrams. The selection of this special set of diagrams and the limiting procedure in extracting the leading terms are not easy to justify in a mathematically sound fashion. They are, as we now proceed to show, at least consistent with gauge invariance, which is a nontrivial condition.

The consistency with gauge invariance may be viewed as two requirements. First, if there is an external photon line having its polarization lying along its four-momentum, the amplitude must vanish. Second, when a term proportional to q_μ and/or q_ν is added to the photon propagator (of momentum q), the final answer must not change.

These requirements set a definite criterion for selecting diagrams. This fact is clear if we remember an important step in the usual derivation of Feynman rules. Recall that, in the propagator for a transverse photon, there are extra terms proportional to q_μ and q_ν besides $-g_{\mu\nu}(q^2-\mu^2+i\epsilon)^{-1}$. Gauge invariance implies that these extra terms do not contribute to the scattering amplitude. The proof of the fact that they indeed do not contribute is well presented in text books.[7] It involves attaching an extra photon vertex *in all possible ways* to any continuous electron line (either a loop or a line with spinors at ends) in a given diagram and showing that the *sum* of the diagrams thus obtained vanishes, if this extra photon, internal or external, has its polarization along its four-momentum. The important point illustrated here is that, to ensure gauge invariance, it is necessary to sum a whole set of diagrams generated in a well-defined way. It follows that the way to generate diagrams consistent with gauge invariance is to permute the photon vertices on each continuous electron line in all possible ways. The diagrams we have selected obviously conform to this rule and are therefore consistent with gauge invariance. An example of diagrams violating this rule is the set of ladder diagrams, which we discussed in Sec. V.

[7] See, for example, J. D. Bjorken and S. D. Drell, *Relativistic Quantum Fields* (McGraw-Hill Book Co., New York, 1965), p. 197.

Although the set of diagrams which we have summed is selected in a way consistent with gauge invariance, it is not automatically guaranteed that our final results are gauge-invariant. This is because we have taken the $s\to\infty$ limit inside the loop integrals and such a limiting process might have rendered the results not gauge-invariant. We now proceed to show that gauge invariance is indeed preserved.

We have calculated the scattering amplitudes with the photons having transverse polarizations. To show that our results are gauge-invariant, we must show that the amplitudes, calculated using the same limiting process, in fact vanish whenever a photon has its polarization along its momentum.

It is sufficient to show that, if the factor $I_{ij}'(\mathbf{k}_1,\mathbf{k}_2)$ [see (7.13)–(7.15)] occurring in the γe and $\gamma\gamma$ amplitudes is replaced by

$$(p-\tfrac{1}{2}k)^\mu I_{\mu j}'(\mathbf{k}_1,\mathbf{k}_2)\,, \tag{7.16}$$

then these scattering amplitudes will vanish. Equation (7.16) is related to the loop integral through

$$I_{\mu j}'(\mathbf{k}_1,\mathbf{k}_2)=I_{\mu j}(\mathbf{k}_1,\mathbf{k}_2)-I_{\mu j}(\mathbf{k},0) \tag{7.17}$$

and

$$(p-\tfrac{1}{2}k)^\mu I_{\mu j}(\mathbf{k}_1,\mathbf{k}_2)\sim(p-\tfrac{1}{2})^\mu\int d^4w M_{\mu j}(\mathbf{k}_1,\mathbf{k}_2;w)\,, \tag{7.18}$$

where $\mathbf{k}_1+\mathbf{k}_2=\mathbf{k}$ and $M_{\mu j}$ is defined by (4.14) with the factor ϵ_i^μ removed.

We wish to emphasize that one has to be careful about the limit $s\to\infty$. To show that our final result is gauge-invariant, we *first* factor out the s dependence in (7.18) and then verify that the remaining coefficient of $\sqrt{s}$ in (7.16) vanishes. The verification of gauge invariance without first taking the limit $s\to\infty$ is trivial, and does not serve as a useful test of our limiting procedure.

In terms of variables in the standard frame, (7.18) leads to

$$(p-\tfrac{1}{2}k)^\mu M_{\mu j}(k_1,k_2;w)=s\epsilon_j'^\nu\,\mathrm{Tr}[S_F(w'-p')$$
$$\times(\not{p}'-\tfrac{1}{2}\not{k})S_F(w'-\tfrac{1}{2}k)\gamma_+S_F(w'-q')\gamma_\nu$$
$$\times S_F(w'-q'-p'-\tfrac{1}{2}k)\gamma_+], \tag{7.19}$$

where

$$q_\pm'=s^{\mp1/2}q_\pm\,,\quad \mathbf{q}'=\mathbf{q}\,.$$

We have written $\mp q+\frac{1}{2}k$ for k_1 and k_2, respectively. The denominators of $S_F(w'-q')$ and $S_F(w'-q'-p'-\frac{1}{2}k)$ contribute a $1/\sqrt{s}$ factor as shown by (4.17)–(4.23). Hence (7.19) has an explicit $\sqrt{s}$ dependence. For the remaining s-independent factors, we note that the first three factors in the trace of (7.19) may be written as the difference

$$S_F(w'-p')-S_F(w'-\tfrac{1}{2}k)\,. \tag{7.20}$$

Substituting (7.20) in (7.19), one proceeds in the same manner as in Sec. IV. The algebra is much simpler. The w_-' integral is then trivial, and the trace can be

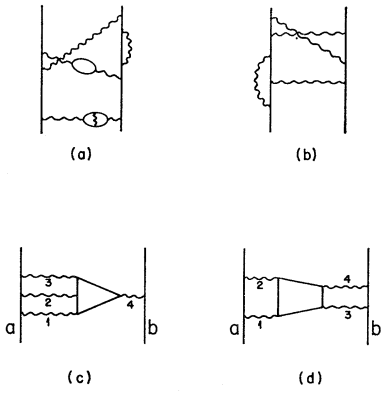

FIG. 10. (a) Self-energy corrections; (b) vertex corrections; (c) and (d) electron loop corrections.

evaluated easily. We have

$$(p-\tfrac{1}{2}k)^{\mu}\int d^4w\, M_{\mu j}(\mathbf{k}_1,\mathbf{k}_2;w)(2\pi)^{-4}i=16i(\sqrt{s})\delta(k_{1-})$$

$$\times\int_0^1 dw_+'(w_+'-\tfrac{1}{2})\int\frac{d^2w}{(2\pi)^2}\frac{(w-Q)^j}{(\mathbf{w}-\mathbf{Q})^2+m^2}, \quad (7.21)$$

$$\mathbf{Q}=\tfrac{1}{2}(w_+'-1)\mathbf{k}_1+\tfrac{1}{2}(w_+'+1)\mathbf{k}_2.$$

This result can be shown to be valid also for the case when one of the $\mathbf{k}_1$ and $\mathbf{k}_2$ vanishes. One can carry out the d^2w integrals in (7.21) explicitly, assuming a circular domain for the integration. The result is proportional to k^j and independent of $\mathbf{k}_1$ or $\mathbf{k}_2$. Therefore,

$$(p-\tfrac{1}{2}k)^{\mu}I_{\mu j}(\mathbf{k}_1,\mathbf{k}_2)\sim k_j$$

or

$$(p-\tfrac{1}{2}k)^{\mu}I_{\mu j}'(\mathbf{k}_1,\mathbf{k}_2)=0,$$

i.e., the longitudinal component of the photon does not contribute to the scattering amplitudes according to our previous conclusion. We have thus demonstrated the gauge invariance of our results.

VIII. DISCUSSION

An interesting feature of our results is the appearance of the eikonal form. As mentioned in the Introduction, in analogy to the high-energy Regge form the eikonal form of the scattering amplitude is first derived from the nonrelativistic potential scattering theory. The most often quoted relativistic model having Regge behavior is the scalar-meson theory in which one sums the ladder diagrams in the t channel. Our result, which is the sum of multiphoton exchange diagrams in the s channel, seems to be the first example of the eikonal form derived from a relativistic field theory.

Thus, in the language of diagrams, the eikonal approximation and the Regge theory reflect the special features of two different categories of diagrams. Without further model calculations and experimental justifications, it is difficult to say which feature is more relevant to high-energy scattering in general.

Clearly, our results cannot be regarded as the exact expressions for the QED amplitudes at infinite energy. As was mentioned in the Introduction, for the time being, we can only demonstrate prominent features of special sets of diagrams. We are very far from being able to analyze all diagrams to get the exact results. An interesting question to ask now is how the above results are modified when diagrams of next higher order in complexity are included.

The diagrams we have summed are skeleton diagrams. The next natural step is to insert self-energy parts into the propagators and make radiative corrections to the vertices. Figures 10(a) and 10(b) show some examples.

The self-energy insertions can be done easily by using the spectral representation of the propagators. For every propagator, one integrates over the mass spectrum. The s dependence of the amplitudes should not change. The photon mass μ appears in the function $\chi(\mathbf{b})$. The integration over μ weighted by the photon spectral function effectively introduces a (momentum-transfer-dependent) dielectric constant of the vacuum in addition to a part which can be removed by renormalization. The electron mass remains only in the propagators adjacent to the external photon lines and gives rise to the mass dependence of I_{ij}. In all the other electron propagators, the mass disappears in the $s\to\infty$ limit. Thus, the integrations over the electron mass spectrum will modify the structure of I_{ij} in addition to the charge and wave-function renormalizations. Of course, the renormalization must be carried out together with the vertex corrections.

The vertex correction is more complicated because it has no spectral representation comparable in simplicity to those for the propagators. Rough estimates show that vertex corrections do not change the s dependence. The amplitude of Fig. 10(b), for example, is still proportional to s. The summation of corrections to all the vertices in Fig. 1 has not yet been carried out.

When one or more electron bubbles are involved in a vertex correction or in more complicated diagram [see Figs. 10(c) and 10(d), for example], additional care is needed in applying the infinite-momentum technique. Consider Fig. 10(c). In the infinite-s limit, it is quite clear that the two electron lines a and b carry infinite and opposite momenta and the photon 4 has a finite momentum. It is not so clear, however, when additional electron loops occur. For example, the photons 1–3 and the bubble can either move with infinite momentum along with electron a or have a finite momentum. Similarly, in Fig. 10(d), the bubble and the photons 1 and 2 can move with infinite momentum along with electron a while the momenta of 3 and 4 stay finite, or the bubble and the photons 3 and 4 can go along with electron b with infinite momenta, leaving 1 and 2 with finite momenta. Furthermore, the bubble and the four

photons can all have finite momenta. When the limit $s \to \infty$ is taken, all cases must be taken into account. A rough estimate shows that, in all cases, these diagrams are of order s (up to $\ln s$). We have not yet obtained conclusive results from these diagrams. It is doubtful that the simple eikonal form of the scattering amplitudes will remain after the vertex correction and more complicated diagrams are included.

Rough estimates show that there are no diagrams which give rise to amplitudes larger than $s(\ln s)^n$ as $s \to \infty$. In fact, we have not encountered in summing the multiphoton exchange diagrams any amplitude which goes like $s(\ln s)^n$, $n \geq 1$, other than those diagrams which are known to violate gauge invariance. Unfortunately, it seems necessary to analyze a diagram in some detail before one can be sure whether such $s \ln s$ terms occur.

The calculation of more complicated diagrams is very involved. But taking the limit $s \to \infty$ before integrating should make the calculation much simpler than the usual way of calculating Feynman amplitudes. What we need is a mathematically more rigorous and technically tractable method for justifying the limiting process. We feel that an extensive study of the infinite-momentum technique is certainly worthwhile, not only for more efficient QED calculations, but also for applications in other areas of physics.

After the completion of this paper, we learned that similar results have also been obtained by Cheng and Wu, by Levy and Sucher, and by Englert *et al.*[8]

ACKNOWLEDGMENTS

We are grateful to Professor Stephen Adler for suggesting this problem and for many helpful comments. We are indebted to Professor Claude Itzykson and Professor Henry Abarbanel for helpful discussions. A conversation with Professor Tai Tsun Wu is gratefully acknowledged.

APPENDIX A

Let $\psi_\lambda(p)$ denote the wave function of a physical one-particle state with momentum $\mathbf{p}=(p^1,p^2)$, $p^3=P\to\infty$, mass m, and helicity λ. Then the wave function in the standard frame is

$$\phi_\lambda(p')=e^{i\xi K_3}\psi_\lambda(p), \tag{A1}$$

with

$$\xi=\ln(p_+/p_+'), \tag{A2}$$

where K_3 is the generator of the Lorentz transformation along the 3 axis and p' is the momentum in the standard frame given by

$$\mathbf{p}'=\mathbf{p}', \quad p_+'=\text{finite}. \tag{A3}$$

Note that $\phi_\lambda(p')$ is *not* an eigenstate of helicity λ with respect to p'; it is a state simply related to the helicity state at infinite momentum.

It is easy to see that the wave function $\psi_\lambda(p)$, in the limit $P\to\infty$, is related to the wave function in the rest frame $\psi_\lambda{}^R$, with λ being the spin along the 3 axis, through

$$\psi_\lambda(p)=\exp[-i(\hat{n}\cdot\mathbf{K})\ln(p_+/m)]\psi_\lambda{}^R, \tag{A4}$$

where $\hat{n}$ is the unit vector along the three-momentum. Then Eq. (A1) can be expressed as

$$\phi_\lambda(p')=e^{i\xi K_3}\exp[-i(\hat{n}\cdot\mathbf{K})\ln(p_+/m)]\psi_\lambda{}^R. \tag{A5}$$

At the limit $P\to\infty$, the right-hand side of (A5) is well defined and leads to[9]

$$\phi_\lambda(p')=e^{-i\mathbf{p}'\cdot\mathbf{X}}e^{-i\ln(p+'/m)K_3}\psi_\lambda{}^R, \tag{A6}$$

where $\mathbf{X}=(X_1,X_2)=(K_1+L_2,\ K_2-L_1)$. The operators $\mathbf{L}$ and $\mathbf{K}$ describe the generators of rotation and accelerations, respectively. Note that $[X_1,X_2]=0$, and that $\mathbf{X}$, L_3, and K_3 form an algebra of $E(2)\otimes D$. Equation (A6) describes the Lorentz transformation between the rest frame and the standard frame. With the help of (A6), it is now quite straightforward to verify (2.13). For Dirac spinors $\psi_\lambda=u_\lambda$, we know that $\mathbf{L}=\frac{1}{2}\sigma$, $K_i=\frac{1}{2}\sigma^{0i}$, and $\mathbf{X}=\frac{1}{2}(\sigma^{01}+\sigma^{31},\ \sigma^{02}+\sigma^{32})$. Using the fact that

$$\begin{aligned}&\mathbf{X}\gamma_+=\gamma_+\mathbf{X}=0,\\ &K_3\gamma_+=-\tfrac{1}{2}i\gamma_+, \quad \gamma_+K_3=\tfrac{1}{2}i\gamma_+,\end{aligned} \tag{A7}$$

we have

$$\begin{aligned}&\bar{u}_1(p_1')\gamma_+u_2(p_2')\\ &=\bar{u}_1{}^Re^{i\ln(p_{1+}'/m)K_3}e^{i\mathbf{p}_1'\cdot\mathbf{X}}\gamma_+e^{-i\mathbf{p}_2'\cdot\mathbf{X}}e^{-i\ln(p_{2+}'/m)K_3}u_2{}^R\\ &=\bar{u}_1{}^Re^{i\ln(p_{1+}'/m)K_3}\gamma_+e^{-i\ln(p_{2+}'/m)K_3}u_2{}^R\\ &=(p_{1+}'p_{2+}')^{1/2}m^{-1}\bar{u}_1{}^R\gamma_+u_2{}^R\\ &=(p_{1+}'p_{2+}')^{1/2}\delta_{\lambda_1\lambda_2}m^{-1},\end{aligned} \tag{A8}$$

which is (2.13). The same technique can be applied to evaluate photon polarizations.

APPENDIX B

In this appendix, we consider the multiphoton exchange diagrams, which we have studied above, for the charged scalar-meson theory. The algebra turns out to be very simple because of the zero spin of the mesons.

The photon vertex now has the form

$$e(p+p')_\mu, \tag{B1}$$

instead of the $e\gamma_\mu$ in QED, where p and p' are the meson momenta on the two sides of the vertex. At infinite s, we have, as before, $\mu=+$ for those vertices on the meson lines with infinite p_+, and $\mu=-$ for those on the meson lines with infinite p_-.

There are also seagull vertices $e^2g_{\mu\nu}$ in addition to (B1). However, in this case μ and ν cannot be both $+$

[8] T. T. Wu (private communication). See also F. Englert *et al.*, Nuovo Cimento (to be published); M. Levy and J. Sucher, Phys. Rev. (to be published). For an alternative derivation, see H. D. I. Abarband and C. Itzykson, Phys. Rev. Letters **23**, 53 (1969); Y. P. Yao (to be published).

[9] H. Bebié and H. Leutwyler, Phys. Rev. Letters **19**, 618 (1967); S. J. Chang, R. Dashen, and L. O'Raifeartaigh, Phys. Rev. **182**, 1805 (1969).

(or both $-$) at the same time. This is because $g_{++}=g_{--}=g_{1\pm}=g_{2\pm}=0$. Therefore, the seagull vertices cannot contribute to the leading term at the $s\to\infty$ limit for the multiphoton exchange diagrams under consideration.

Without the seagull vertices, the algebra is similar to what we have done but much simpler and is left as an exercise for the reader. The results are the following. For the meson-meson scattering amplitude one obtains

$$M(m^-,m^\mp)=\tfrac{1}{2}isF_\pm(\mathbf{k}), \tag{B2}$$

similar to (5.24). For photon-meson and photon-photon scattering amplitudes, we simply replace $\delta_{\lambda\lambda'}/m^2$ in (7.8) by unity and use the new I_{ij} factor

$$I_{ij}(\mathbf{k}_1,\mathbf{k}_2)=-\frac{\alpha}{\pi}\int_0^1 d\beta d\beta' dx\,\delta(1-\beta-\beta') \times 4\beta\beta'[x(1-x)K_iK_j+(x-\tfrac{1}{2})^2\mathbf{K}^2\delta_{ij}] \times[m^2+x(1-x)\mathbf{K}^2]^{-1}, \tag{B3}$$

$$\mathbf{K}\equiv\beta'\mathbf{k}_2-\beta\mathbf{k}_1, \tag{B4}$$

in (7.8) and (7.9). Equation (B3) is only slightly different from (4.33).

PHYSICAL REVIEW VOLUME 188, NUMBER 5 25 DECEMBER 1969

Equal-Time Commutators and Equations of Motion for Current Densities in a Renormalizable Field-Theory Model

WU-KI TUNG
Institute for Advanced Study, Princeton, New Jersey 08540
(Received 14 May 1969)

The equal-time commutators of current densities are studied in a renormalizable field theory. From a careful study of the equations of motion for current densities and products of current densities, a relation between the full commutators and the naive commutators is derived. The difference between the two is related to the well-known seagull terms associated with time-ordered products of currents and to anomalies in the equations of motion for current densities. Previous second-order perturbation calculations on specific matrix elements are shown to be special cases of this general result.

I. INTRODUCTION

A USEFUL way of formulating most of the applications of the usual $SU(3)\otimes SU(3)$ current algebra[1] (and its generalizations) is to start from a formal Ward identity. Recent developments in exploiting an even wider class of local current commutators are based on the Bjorken-limit technique.[2] Both the "Ward identity" and the Bjorken relation are formal relations between equal-time commutators and time-ordered products of current densities. In all the applications, one assumes certain algebraic structure for the current commutators (usually obtained by naive use of canonical commutation relations) and deduces its consequences on the time-ordered products. For theoretical purposes, it is also desirable to study the inverse problem. Given a theory in which the time-ordered products can be calculated, one can use these same formal relations to define the current commutators. These can then be compared with the usually assumed naive commutators. One thus obtains a check on the reliability of the results which are deduced from the assumed commutators.

This latter point of view was first adopted by Johnson and Low,[3] who calculated a particularly simple matrix element of a large class of current commutators to the lowest order in perturbation theory. Although their results show that the simple commutators usually assumed are not always the full commutators in their model, the anomalies do not directly invalidate any of the usual applications of the assumed current commutators. Recent calculations along the same line but on more physical matrix elements show that additional anomalies exist and that almost all the principal applications of the Bjorken-limit technique do not hold in second-order perturbation theory.[4–6]

[1] For a comprehensive review, see S. L. Adler and R. F. Dashen, *Current Algebras* (W. A. Benjamin, Inc., New York, 1968).
[2] J. D. Bjorken, Phys. Rev. **148**, 1467 (1966).
[3] K. Johnson and F. E. Low, Progr. Theoret. Phys. (Kyoto) Suppl. **37-38**, 74 (1966).
[4] A. I. Vainshtein and B. L. Jaffe, Zh. Eksperim. i Teor. Fiz. **6**, 917 (1967) [English transl.: Soviet Phys.—JETP **6**, 34 (1967)]. These authors calculated the virtual Compton scattering in the pseudoscalar gluon model and found that the violation of Eq. (9) is accompanied by logarithmic divergences. They concluded that the failure of Eq. (9) to hold is due to the infinities encountered. This conclusion is contradicted by the results of Ref. 6.
[5] R. Jackiw and G. Preparata, Phys. Rev. Letters **22**, 975 (1969); **22**, 1162(E) (1969); and to be published. These authors calculated the spin-averaged forward Compton-scattering amplitude in the vector gluon model. In this case the first term in Eq. (7) vanishes. What is tested is the commutator $[\dot{V}_i,V_j]$. Again, the violation of Eq. (9) is accompanied by logarithmic divergence and the authors reached the same conclusion as that reached in Ref. 4.
[6] S. L. Adler and Wu-Ki Tung, Phys. Rev. Letters **22**, 978 (1969); and to be published. In addition to the case $[\dot{V}_i,V_j]$, it is shown here that in the vector gluon model, Eq. (9) is violated for all commutators involving V_i and A_i even if all quantities involved are finite and well defined.